



HAL
open science

Major proteome variations associated with cherry tomato pericarp development and ripening

Mireille Faurobert, Christina Mihr, Nadia Bertin, Tomasz Pawlowski, Luc Négroni, Nicolas Sommerer, Mathilde M. Causse

► To cite this version:

Mireille Faurobert, Christina Mihr, Nadia Bertin, Tomasz Pawlowski, Luc Négroni, et al.. Major proteome variations associated with cherry tomato pericarp development and ripening. *Plant Physiology*, 2007, 143 (3), pp.1327-1346. 10.1104/pp.106.092817 . hal-02667189

HAL Id: hal-02667189

<https://hal.inrae.fr/hal-02667189>

Submitted on 31 May 2020

HAL is a multi-disciplinary open access archive for the deposit and dissemination of scientific research documents, whether they are published or not. The documents may come from teaching and research institutions in France or abroad, or from public or private research centers.

L'archive ouverte pluridisciplinaire **HAL**, est destinée au dépôt et à la diffusion de documents scientifiques de niveau recherche, publiés ou non, émanant des établissements d'enseignement et de recherche français ou étrangers, des laboratoires publics ou privés.

Major Proteome Variations Associated with Cherry Tomato Pericarp Development and Ripening^[OA]

Mireille Faurobert*, Christina Mihr, Nadia Bertin, Tomasz Pawlowski, Luc Negroni, Nicolas Sommerer, and Mathilde Causse

Institut National de la Recherche Agronomique, Unité de Génétique et Amélioration des Fruits et Légumes, INRA, UR 1052, Domaine Saint-Maurice, 84143 Montfavet cedex, France (M.F., C.M., M.C.); Institut National de la Recherche Agronomique, Unité Plantes et Systèmes de Culture Horticoles, INRA, UR 1115, Domaine Saint-Paul, 84914 Avignon cedex 9, France (N.B.); Instytut Dendrologii, Polska Akademia Nauk, 62–035 Kornik, Poland (T.P.); Institut National de la Recherche Agronomique, Unité Mixte de Recherche de Génétique Végétale, Institut Fédératif de Recherche 87, Plate-Forme de Protéomique du Moulon, 91190 Gif-sur-Yvette, France (L.N.); and Institut National de la Recherche Agronomique, Unité de Recherches Protéomique, INRA, UR 1199, 34000 Montpellier, France (N.S.)

Tomato (*Solanum lycopersicum*) is a model plant for studying fleshy fruit development. Several genetic and molecular approaches have been developed to increase our knowledge about the physiological basis of fruit growth, but very few data are yet available at the proteomic level. The main stages of fruit development were first determined through the dynamics of fruit diameter and pericarp cell number. Then, total proteins were extracted from pericarp tissue at six relevant developmental stages and separated by two-dimensional gel electrophoresis. Protein patterns were markedly different between stages. Proteins showing major variations were monitored. We identified 90 of 1,791 well-resolved spots either by matrix-assisted laser-desorption ionization time-of-flight peptide mass fingerprinting or liquid chromatography-mass spectrometry sequencing and expressed sequence tag database searching. Clustered correlation analysis results pointed out groups of proteins with similar expression profiles during fruit development. In young fruit, spots linked to amino acid metabolism or protein synthesis were mainly expressed during the cell division stage and down-regulated later. Some spots linked to cell division processes could be identified. During the cell expansion phase, spots linked to photosynthesis and proteins linked to cell wall formation transiently increased. In contrast, the major part of the spots related to C compounds and carbohydrate metabolism or oxidative processes were up-regulated during fruit development, showing an increase in spot intensity during development and maximal abundance in mature fruit. This was also the case for spots linked to stress responses and fruit senescence. We discuss protein variations, taking into account their potential role during fruit growth and comparing our results with already known variations at mRNA and metabolite-profiling levels.

Tomato (*Solanum lycopersicum*) is one of the most consumed vegetables in the world and it plays an important role in the human diet. Tomato has long served as a model system for plant genetics, development, physiology, pathology, and fleshy fruit ripening, resulting in the accumulation of substantial information regarding the biology of this economically important organism. Many genomic tools are now available on this Solanaceous species and have rapidly generated a great amount of genomic resources, including mapping populations, mapped DNA markers, bacterial artificial chromosomes, and expressed sequence tag (EST) collections (Giovannoni, 2004). There are

currently 184,000 tomato ESTs available (37,000 fruit ESTs) that have allowed the identification of approximately 30,000 unigenes across a range of tissues and developmental stages. Numerous mutants exist concerning fruit development and ripening and genome sequencing is under way (Mueller et al., 2005). Gene expression profiling of fruit development and maturation was recently examined (Fei et al., 2004; Alba et al., 2005; Lemaire-Chamley et al., 2005). An increasing number of data are now available from large-scale analysis of gene expression during climacteric or non-climacteric fruit development (Aharoni and O'Connell, 2002; Hennig et al., 2004; da Silva et al., 2005; Grimplet et al., 2005; Moyle et al., 2005; Terrier et al., 2005).

However, only few data on fruit development proteomics are available (Sarry et al., 2004; Rocco et al., 2006). Similar to gene expression profiling, proteomics offers the opportunity to examine simultaneous changes and to classify temporal patterns of protein accumulation occurring in complex developmental processes (Cánovas et al., 2004). Moreover, the proteome reflects the expression of molecules that directly influence

* Corresponding author; e-mail mireille.fauRobert@avignon.inra.fr; fax 33-4-32-72-27-02.

The author responsible for distribution of materials integral to the findings presented in this article in accordance with the policy described in the Instructions for Authors (www.plantphysiol.org) is: Mireille Faurobert (mireille.fauRobert@avignon.inra.fr).

^[OA] Open Access articles can be viewed online without a subscription.

www.plantphysiol.org/cgi/doi/10.1104/pp.106.092817

cellular biochemistry. As compared with the RNA level, the protein level integrates posttranscriptional and posttranslational processing that modulates the quantity, localization, and efficiency of the final product in the cell. This information can thus be included with the annotation of the corresponding gene (Baginsky and Grissem, 2006). Proteomic data can be useful in genome annotation improvement, particularly by confirming intron-exon boundaries or the existence of splice variants (Desiere et al., 2004). As previously noted, some discrepancies between proteins and their specific mRNA can exist (Rose et al., 2004). Coupling transcriptomic with proteomic studies will lead to better knowledge of gene networks. Finally, integrating the metabolome level is essential to decipher complex biological systems (Fernie et al., 2004). In terms of fruit development, data on metabolome profiling are now available (Schauer et al., 2005; Carrari et al., 2006; Carrari and Fernie, 2006).

The development of tomato fruit can be divided into two distinct phases. During the first phase, which lasts for about 7 to 10 d after fertilization, a very active period of cell division occurs within the pericarp, mainly in the outer layer (Gillaspy et al., 1993; Joubès et al., 1999). After this phase, the fruit size increase is related to a considerable cell expansion rate that involves not only cell wall expansion, but also synthesis of new cell wall material (Brummell and Harpster, 2001). Ripening is initiated after these two phases because seed maturation has been completed. It is characterized by fruit softening, coloring, and sweetening. In climacteric fruit, such as tomato, it is preceded by a dramatic increase in ethylene production (Giovannoni, 2001, 2004; Adams-Phillips et al., 2004).

This work was undertaken to explore the potential of proteomic investigations into fruit development and ripening. It provides a detailed framework of pericarp protein patterning during fruit development, describing the main fruit pericarp proteome variations at precise stages of tomato fruit development and ripening. Comparative analysis of the fruit pericarp proteome was performed during the cell division, cell expansion, and fruit-ripening stages. Our main objectives were to (1) investigate the dynamic nature of the protein network in relation to fruit development; (2) identify the most variable proteins within the pericarp in total protein extraction conditions; and (3) link the protein variations with major phases of fruit development on the basis of their physiological role.

RESULTS

Identification of the Developmental Stages of Cherry Tomato

Our proteomic analysis was anchored with proper stages of tomato fruit development. We followed fruit growth by measuring either the equatorial fruit diameter or the fruit fresh weight increase (Fig. 1A). Cervil

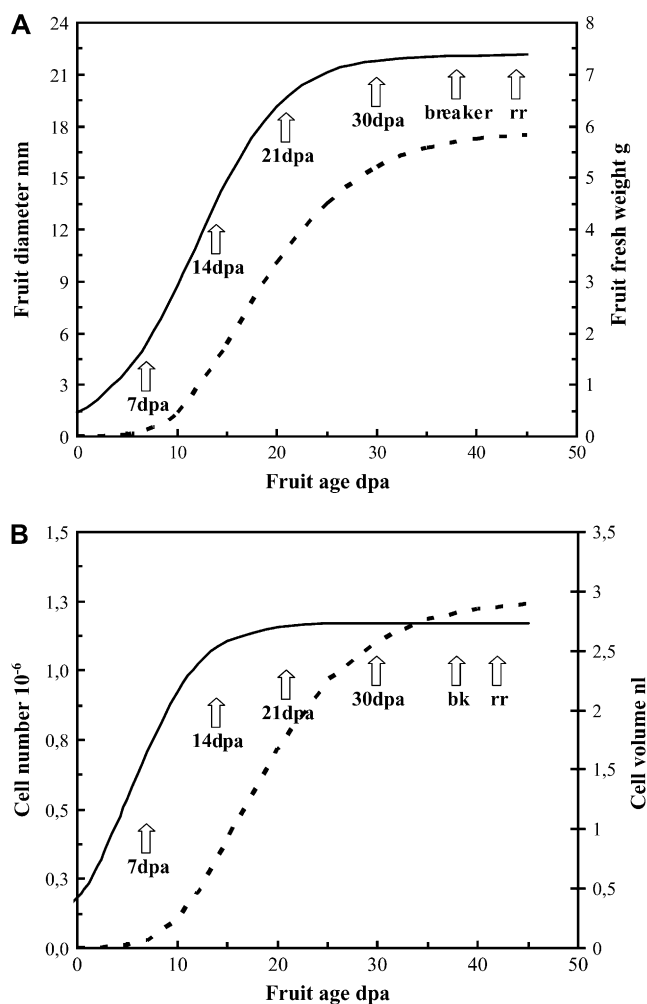


Figure 1. Kinetics of cherry tomato fruit growth. A, Fruit growth estimated by measurement of equatorial fruit diameter and fresh weight. The equatorial fruit diameter (left y axis, solid line) and fruit fresh weight (right y axis, dotted line) are given as a function of fruit age (DPA). Curves were fitted to three-parameter Sigmoid and Gompertz functions for the diameter ($n = 497$; $R^2 = 0.97$) and fresh weight ($n = 497$; $R^2 = 0.94$). B, Dynamics of pericarp cell number ($\times 10^6$) and mean cell volume (nL) as a function of fruit age (DPA). Each point is the average of eight measurements made on one individual fruit. All fruits were sampled at different positions (basal and tip) within the third inflorescence. Curves were fitted to three-parameter Sigmoid and Gompertz functions for the number ($n = 65$; $R^2 = 0.91$) and size ($n = 65$; $R^2 = 0.97$) of cells, respectively. Arrows indicate the sampling dates.

fruit growth included two phases. Intensive fruit growth started between 5 and 8 d post anthesis (DPA) and reached a plateau between 25 and 30 DPA. Mean final fruit size and fresh weight were, respectively, 22 mm and 5.8 g. The initial phase of growth was characterized first by intensive cell division within the pericarp from 0 to 10 DPA (Fig. 1B). Divisions ended around 14 DPA to reach a final number of 1.17×10^6 cells. Then, from 10 to 25 DPA, intensive cell expansion took place. The final cell volume was 2.9 nL, on average, which would correspond to a mean cell diameter of 168 μm if

cells are considered to be spherical. Ripening occurred between 30 and 40 DPA.

For this proteomic study, sampling was performed at 7 DPA to study the division phase, 21 DPA for the cell expansion phase, and at the mature stage corresponding to red ripe (RR) fruit. Fourteen DPA, 30 DPA, and breaker stages were also sampled to investigate overlapping stages between the three phases. At 14 DPA, some cell divisions still occurred when intensive expansion was settled. Thirty DPA corresponded to the end of cellular expansion; at this stage, fruit growth had stopped and fruit was able to ripen (data not shown). The breaker stage corresponded to an intermediate stage between the expansion phase and the RR stage. This stage was marked by fruit color change from green to red.

Proteome Maps of Tomato Pericarp during Fruit Development

Protein content varied throughout fruit development. It represented 0.23%, on average, of the pericarp fresh weight 7 DPA; later, it decreased to 0.085% until the breaker stage, where it reached 0.1%. Two-dimensional electrophoresis (2-DE) gels of the six different developmental stages were compared (Fig. 2). The total number of detected spots varied according to the developmental stage. From 7 to 21 DPA, gels exhibited fewer spots (1,415, on average) and spots showed higher M_r than from 30 DPA to the RR stage (1,730 spots, on average). To construct the pericarp master gel, we chose one image of a breaker-stage gel as a reference and then we added the spots specifically detected on the reference gels of the other stages. Finally, 1,791 different spots were taken into account to create this synthetic master gel. As expected, the

number of detected spots was higher in silver-stained gels than on Coomassie Blue gels, where 550, on average, were detected.

Identification of Variable Spots

A total of 148 spots were significantly variable (ANOVA) as detected by using IMAGE MASTER platinum, version 5, representing about 8% of the spots on the master gel. Only 90 of them were also present on the Coomassie Blue-stained gels and were excised from polyacrylamide gels for mass spectrometry (MS) identification by matrix-assisted laser-desorption ionization (MALDI)-time-of-flight (TOF). All searches were done against the MS protein sequence database (MSDB) and The Institute for Genomic Research (TIGR) tomato tentative consensus (TC) database. In each case, annotations were similar. Sixty-five percent of spots were successfully identified by MALDI-TOF, the remaining spots being identified by liquid chromatography (LC)-tandem MS (MS/MS) and TIGR database searching. The discrepancy between the two methods can largely be attributed to the lack of a genome sequence database. Our results clearly confirm the usefulness of a large and well-annotated tomato EST database to achieve a high rate of protein identification through MS/MS analysis. In the future, the tomato genome sequence will provide a basic tool for improved protein identification (Mueller et al., 2005).

Data obtained for these spots are presented in Table I and spot positions are illustrated on Cervil gel at the breaker stage in Figure 3. Unambiguous results were obtained for MALDI-TOF analysis, percentages of sequence covering ranged from 13% to 75%, and also for LC-MS/MS experiments, the number of obtained peptides varied from 3 to 17 and the number of amino

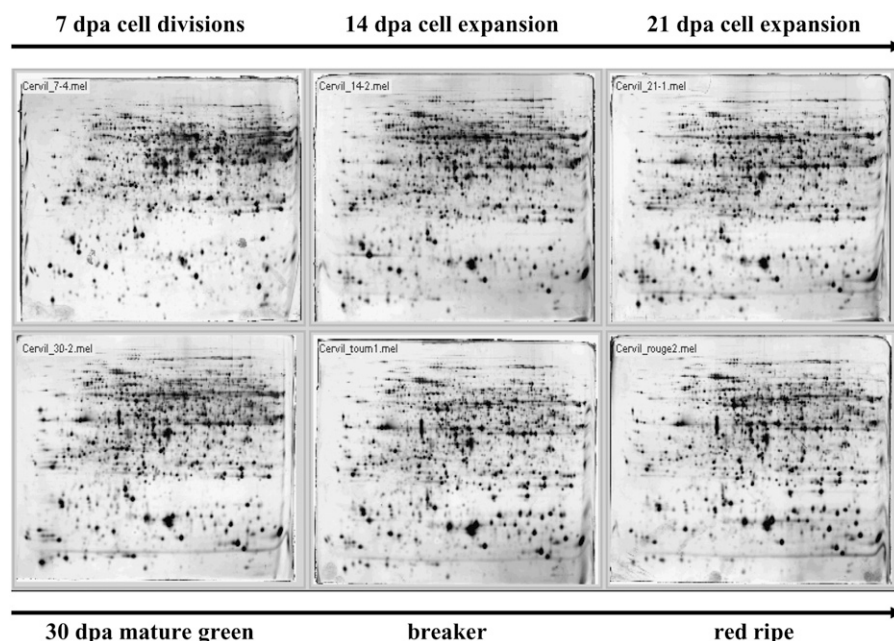


Figure 2. Representative silver-stained 2-DE gels of cherry tomato fruit pericarp proteome variation during fruit growth. Gels were performed from 100 μg of proteins using 24-cm immobilized pH gradient strips (linear pH 4–7). From 7 DPA to the RR stage, gels showed altered patterns, with increasing spot number ranging from 1,415 to 1,730 spots and a shift from high to lower M_r . Numerous individual spot intensity variations were noticed.

Table 1. Functional classification of tomato proteins whose level varied significantly during fruit development and ripening

List of identified proteins from pericarp tissues of Cervil. Data were classified according to the FunCat scheme. For each spot, the computed and theoretical pIs and M_r and the mean normalized volume at the six stages of development were indicated.

Spot No. ^a	MS ^b	Database	Accession No. ^c	Coverage ^d	Peptides Identified ^e	UniProt Accession No.	Assignment	Species	Computed		Observed		Mean % Volume ^f					
									pI	M_r	pI	M_r	7 DPA	14 DPA	21 DPA	30 DPA	Breaker	RR
%																		
C compounds and carbohydrate metabolism																		
108	M	MSDB	Q42896	61	21/33	Q42896	Fructokinase Frk2	<i>Lycopersicon esculentum</i>	5.76	34.8	6.15	36	50.75	36.31	26.64	15.02	8.43	6.79
100	M	MSDB	Q9AV98	21	16/53	Q6IVK5	UDP-glucuronate decarboxylase 1	Tobacco	7.10	38.7	6.6	45	8.21	19.73	13.44	12.18	8.02	8.11
10	E	TIGR	BF050929	na	5	Q8W147	Putative kunitz-type tuber invertase inhibitor precursor	Potato	8.22	24.5	5.98	27	43.23	22.82	12.66	16.51	15.05	19.37
118	E	TIGR	TC162820	na	14	Q9LQ04	3,5-Epimerase/4-reductase	Arabidopsis	5.73	33.6	6.49	32	6.64	6.22	5.35	3.94	2.29	1.29
57	M	TIGR	TC153775	na	8/27	Q94CE4	Similar to carbonic anhydrase	Arabidopsis	6.66	30.8	6.07	29	2.30	1.76	6.08	3.11	9.16	11.31
6	M	MSDB	S31157	34	14/23	P29000	Acid β -fructofuranosidase precursor	<i>L. esculentum</i>	5.31	70.1	5.87	30	4.86	6.17	12.35	15.02	22.81	43.96
73	E	TIGR	TC161907	na	6	P29000	Acid β -fructofuranosidase precursor	<i>L. esculentum</i>	5.31	70.1	5.74	21	0.00	4.69	2.86	4.44	6.29	33.20
74	M	TIGR	AAL75449	21	8/11	P29000	Acid β -fructofuranosidase precursor	<i>L. esculentum</i>	5.54	70.1	5.69	20	0.00	4.40	6.69	4.92	9.31	31.21
75	M	TIGR	AAL75449	22	9/18	P29000	Acid β -fructofuranosidase precursor	<i>L. esculentum</i>	5.54	70.1	5.7	20	7.68	3.23	3.75	5.40	7.43	15.34
115	M	MSDB	S31157	18	14/21	P29000	Acid β -fructofuranosidase precursor	<i>L. esculentum</i>	5.54	70.1	5.67	27	2.93	4.92	3.62	5.07	8.52	8.41
144	M	TIGR	AAL75449	16	7/14	P29000	Acid β -fructofuranosidase precursor	<i>L. esculentum</i>	5.54	70.1	5.82	49	20.74	27.29	36.02	35.72	55.10	62.32
145	M	TIGR	AAL75449	34	17/31	P29000	Acid β -fructofuranosidase precursor	<i>L. esculentum</i>	5.54	70.1	5.9	49	14.41	16.40	21.40	23.72	44.49	47.79
26	M	MSDB	S44364	60	13/30	Q43778	Glucan endo-1,3- β -D-glucosidase	<i>L. esculentum</i>	5.38	37.9	5.73	33	0.00	0.00	1.44	3.89	12.72	12.34
20	E	TIGR	TC154654	na	5	Q76MS4	Xylosidase	<i>L. esculentum</i>	8.04	68.9	6.47	60	3.94	5.88	2.37	7.10	7.35	7.79
133	M	MSDB	Q9FUR8	30	10/21	Q9SP05	α -Galactosidase	<i>L. esculentum</i>	5.3	44.9	5.7	37	4.01	4.63	6.89	6.57	14.67	19.39
Photosynthesis/respiration																		
37	M	MSDB	RKTOS2	33	6/20	P07179	Rubisco small chain 2A	<i>L. esculentum</i>	6.58	20.3	5.84	7	10.17	20.60	35.40	40.55	17.58	14.33
72	M	MSDB	S16586	40	13/23	P26320	PSII oxygen-evolving complex protein 1	Potato	5.84	35.4	5.72	31	26.67	29.17	35.47	26.45	18.83	6.61
138	M	MSDB	T06368	49	13/23	P26320	PSII oxygen-evolving complex protein 1	Potato	5.84	35.4	5.76	31	30.34	31.47	34.32	32.92	26.38	10.89
76	M	MSDB	F2TOX2	43	9/21	P29795	PSII oxygen-evolving complex protein 2	<i>L. esculentum</i>	8.27	27.8	5.75	22	50.28	77.00	69.70	69.31	51.31	27.77
32	E	TIGR	TC158143	na	8	Q6NQE2	At4g27270, similar to 1,4-benzoquinone reductase	Arabidopsis	6.08	21.8	6.12	25	2.42	3.46	5.91	5.83	7.04	8.06

(Table continues on following page.)

Table I. (Continued from previous page.)

Spot No. ^a	MS ^b Database	Accession No. ^c	Coverage ^d	Peptides Identified ^e	UniProt Accession No.	Assignment	Species	Computed		Observed		Mean % Volume ^f							
								pI	M _r	pI	M _r	7 DPA	14 DPA	21 DPA	30 DPA	Breaker	RR		
Amino acid metabolism																			
97	M	TIGR	TC154906	na	11/16	O04130	D-3-Phosphoglycerate dehydrogenase (3-PGDH)	Arabidopsis	5.81	66.5	6.13	60	6.80	4.75	3.63	3.43	1.22	0.00	
99	M	TIGR	TC154906	na	14/19	O04130	D-3-Phosphoglycerate dehydrogenase (3-PGDH)	Arabidopsis	5.81	66.5	6.22	60	6.88	3.37	3.88	3.81	0.00	0.00	
23	M	MSDB	S46540	30	8/16	P43282	S-adenosyl methionine synthetase 3	<i>L. esculentum</i>	5.76	42.7	6.26	46	19.60	9.96	4.71	3.02	1.77	1.22	
109	M	MSDB	S46540	34	11/34	P43282	S-adenosyl methionine synthetase 3	<i>L. esculentum</i>	5.76	42.7	6.2	45	19.99	12.44	8.96	6.65	2.88	2.38	
147	M	MSDB	S46540	37	12/14	P43282	S-adenosyl methionine synthetase 3	<i>L. esculentum</i>	5.76	42.7	6.34	45	10.18	7.00	2.82	2.27	1.28	1.02	
105	E	TIGR	TC164711	na	3	Q9FFW8	Trp synthase β -chain	Arabidopsis	6.79	55.7	6.53	50	3.61	5.85	3.99	6.41	4.02	2.64	
22	M	MSDB	Q9XGI9	46	9/35	Q9XGI9	β -Alanine synthase	<i>L. esculentum</i>	5.87	33.4	6.25	33	0.00	1.32	3.52	3.26	3.58	3.34	
102	E	TIGR	TC162607	na	12	P50217	Homolog to NADP ⁺ -specific isocitrate dehydrogenase	Potato	6.54	46.8	6.61	37	2.00	2.12	2.56	1.57	2.70	4.71	
103	M	MSDB	S47013	37	15/40	P50217	Homolog to NADP ⁺ -specific isocitrate dehydrogenase	Potato	6.54	46.8	6.6	45	1.47	1.94	1.93	1.65	6.37	9.05	
Protein synthesis/storage																			
16	E	TIGR	TC162231	na	5	Q9AXQ5	eIF-5A 2	<i>L. esculentum</i>	5.78	17.6	6.12	18	15.34	11.05	1.05	4.30	10.70	5.93	
112	E	TIGR	TC155242	na	8	P19954	Plastid-specific 30S ribosomal protein 1	<i>Spinacia oleracea</i>	6.68	33.7	5.89	33	15.63	13.58	13.98	9.52	5.59	4.30	
15	E	TIGR	TC162122	na	10	Q9AXQ3	eIF-5A 4	<i>L. esculentum</i>	5.6	17.5	5.99	18	17.18	23.44	6.06	7.47	11.85	19.73	
Protein fate, modification, degradation																			
91	M	TIGR	TC162419	na	11/12	Q9XF61	Similar to protein disulfide-isomerase precursor	<i>Datisca glomerata</i>	4.84	57.1	5.5	58	11.14	8.05	8.31	5.28	5.20	3.25	
58	M	MSDB	JQ0988	34	5/11	P54153	Peptide methionine sulfoxide reductase, protein E4	<i>L. esculentum</i>	6.1	21.9	6.19	23	0.00	0.00	0.00	0.00	29.48	46.78	
60	M	MSDB	JQ0988	34	7/15	P54153	Peptide methionine sulfoxide reductase, protein E4	<i>L. esculentum</i>	6.1	21.9	6.39	23	0.00	0.00	0.00	0.99	35.71	51.62	
5	M	MSDB	S66348	30	6/20	Q40143	Cysteine proteinase 3 precursor	<i>L. esculentum</i>	8.59	38.9	5.89	29	4.21	11.35	14.27	23.53	24.44	28.44	
7	E	TIGR	TC153677	na	8	Q9FRW8	Similar to aspartic proteinase 2	<i>Nepenthes alata</i>	5.28	55.4	6.03	31	0.00	1.33	5.87	9.08	6.74	10.14	
Secondary metabolism																			
3	E	TIGR	TC162337	na	14	Q9FES7	Homolog to sulfur (Mg chelatase)	Tobacco	6	46.3	5.72	40	7.06	4.09	4.20	2.32	2.03	0.00	
51	E	TIGR	TC162337	na	17	Q9FES7	Homolog to sulfur (Mg chelatase)	Tobacco	6	46.3	5.65	40	6.14	7.28	5.98	4.75	2.72	0.00	
2	E	TIGR	TC166223	na	9	Q9LHN8	Weakly similar to leucoanthocyanidin dioxygenase-like	Arabidopsis	5.26	40.7	5.75	41	11.81	9.98	7.19	4.68	1.93	1.66	

(Table continues on following page.)

Table I. (Continued from previous page.)

Spot No. ^a	MS ^b Database	Accession No. ^c	Coverage ^d	Peptides Identified ^e	UniProt Accession No.	Assignment	Species	Computed		Observed		Mean % Volume ^f						
								pI	M _r	pI	M _r	7 DPA	14 DPA	21 DPA	30 DPA	Breaker	RR	
67	E	TIGR	TC156069	na	14	Q9FGT8	Similar to outer membrane lipoprotein-like (lipocalin)	Arabidopsis	5.98	21.4	6.34	20	5.02	7.95	8.37	8.43	41.39	45.32
68	E	TIGR	TC156069	na	5	Q9FGT8	Similar to outer membrane lipoprotein-like (lipocalin)	Arabidopsis	5.98	21.4	6.41	20	0.00	0.00	0.00	0.00	25.95	41.78
Vitamin biosynthesis																		
53	M	MSDB	Q9SLR7	22	6/11	Q9SLR7	Thiamin biosynthetic enzyme	<i>Glycine max</i>	5.8	37.0	5.59	34	1.72	7.83	11.76	15.60	0.00	0.00
Lipid metabolism																		
148	M	MSDB	T06339	29	21/43	P38416	Lipoxygenase loxB	<i>L. esculentum</i>	5.56	97.1	6.32	59	2.95	3.58	2.27	4.16	5.28	8.35
DNA processing																		
134	M	TIGR	TC155302	na	10/30	Q94KA9	Homolog to importin α 2	Pepper	5.32	58.5	5.76	56	4.79	10.27	9.05	9.44	8.42	9.66
Stress response																		
126	E	TIGR	TC153554	na	9	P93570	Chaperonin-60 β -subunit	Potato	5.72	63.0	5.88	57	3.70	1.64	1.00	1.07	1.65	1.29
123	E	TIGR	TC162423	na	4	Q8LEG8	Weakly similar to dehydration stress-induced protein	Arabidopsis	5.12	20.0	5.66	16	10.39	26.50	23.18	27.51	18.76	14.92
11	M	MSDB	T04316	58	13/27	O80432	Mitochondrial small HSP	<i>L. esculentum</i>	6.47	23.8	5.61	21	6.69	16.32	9.18	5.66	11.07	18.44
34	M	MSDB	O82010	62	11/18	O82010	HSP 20.1	<i>L. peruvianum</i>	5.83	17.7	5.92	18	9.70	34.36	37.15	71.12	82.64	111.60
120	M	MSDB	O82545	28	5/26	O82013	HSP 20.2	<i>L. peruvianum</i>	6.32	17.3	6.64	17	3.79	18.51	21.88	23.03	38.14	54.40
140	M	TIGR	TC162823	na	14/26	Q39641	Homolog to HSP 70	<i>Cucumis sativus</i>	5.15	75.4	5.46	69	0.00	1.94	3.13	3.45	5.28	5.22
141	M	TIGR	TC162823	na	17/27	Q39641	Homolog to HSP 70	<i>C. sativus</i>	5.15	75.4	5.49	69	1.87	4.14	7.03	6.88	11.48	11.19
146	M	MSDB	JC4786	43	23/44	Q40151	Hsc 70 protein	<i>L. esculentum</i>	5.18	71.5	5.7	67	0.00	6.38	7.18	8.56	12.77	17.20
94	M	MSDB	S53498	18	9/19	Q40980	HSP 70	Pea	5.17	71.2	5.77	68	9.02	5.78	6.90	5.10	20.19	22.93
65	M	TIGR	TC155466	na	8/25	Q6WHC0	Similar to chloroplast small HSP class I	<i>Capsicum frutescens</i>	6.2	18.2	6.61	18	0.00	7.78	10.28	11.64	24.49	33.31
64	E	TIGR	TC162458	na	5	Q84JS5	Similar to At3g58450: universal stress protein family	Arabidopsis	6.09	22.4	6.63	20	0.00	5.89	13.69	18.40	46.17	37.24
18	M	TIGR	TC154685	na	7/20	Q8H0L9	Similar to DS2 protein	<i>Solanum chacoense</i>	4.99	29.1	5.49	62	0.00	1.49	2.84	6.73	5.50	3.08
85	M	TIGR	TC154685	na	13/20	Q8H0L9	Similar to DS2 protein	<i>S. chacoense</i>	4.99	29.1	5.52	62	0.78	3.77	6.93	12.36	11.93	6.37
58c	M	MSDB	T06324	40	9/15	Q95661	Small HSP, chloroplast HSP21 TOM111	<i>L. esculentum</i>	7.84	26.2	6.2	22	0.00	0.00	0.00	0.00	3.66	6.34
63	E	TIGR	TC160055	na	3	Q9LS37	Small HSP	<i>L. esculentum</i>	5.89	21.5	6.49	20	0.00	4.58	8.21	4.37	28.85	42.80
66	M	MSDB	Q9LS37	37	8/45	Q9LS37	Small HSP	<i>L. esculentum</i>	5.89	21.5	6.23	20	5.28	11.61	11.51	6.18	39.07	57.11
55	E	TIGR	TC165474	na	8	Q9SSQ8	Weakly similar to 26.5-kD class I small HSP-like	Arabidopsis	6.86	26.5	5.97	25	0.00	3.41	4.78	6.12	23.33	39.65
59	E	TIGR	TC165474	na	5	Q9SSQ8	Weakly similar to 26.5-kD class I small HSP-like	Arabidopsis	6.86	26.5	6.17	25	3.77	7.32	5.81	5.13	19.18	20.79
121	M	MSDB	Q9SYU8	75	15/29	Q9SYU8	17.7-kD class I small HSP	<i>L. esculentum</i>	5.84	17.7	6.09	19	10.10	29.77	27.31	40.69	89.14	94.40
Disease/defense																		
4	M	TIGR	AW040299	na	8/21	P49248	Similar to In2-1 protein	Maize	4.80	27.0	5.5	29	17.71	5.64	2.81	2.08	0.82	0.00

(Table continues on following page.)

Table I. (Continued from previous page.)

Spot No. ^a	MS ^b Database	Accession No. ^c	Coverage ^d	Peptides Identified ^e	UniProt Accession No.	Assignment	Species	Computed		Observed		Mean % Volume ^f							
								pI	M _r	pI	M _r	7 DPA	14 DPA	21 DPA	30 DPA	Breaker	RR		
49	E	TIGR	AW040299	na	8	P49248	Similar to In2-1 protein	Maize	4.80	27.0	5.76	42	8.31	12.62	9.82	9.31	3.01	1.54	
78	E	TIGR	TC156701	na	3	Q6RYA0	Similar to salicylic acid-binding protein 2	Tobacco	5.39	29.3	6.16	29	6.42	7.91	5.54	3.45	4.39	14.10	
Detoxification																			
89	M	MSDB	T07747	48	6/28	O24032	Glutathione peroxidase GPXle-2	<i>L. esculentum</i>	5.13	11.2	5.64	20	37.96	14.27	9.89	7.65	8.45	9.04	
122	E	TIGR	TC154854	na	6	Q7XAV2	SOD	<i>L. esculentum</i>	6.01	22.3	6.03	15	14.15	16.44	13.91	14.63	9.89	10.28	
14	M	TIGR	TC162330	na	5/20	Q7F8S5	Similar to putative thioredoxin peroxidase	Rice	6.15	23.2	5.44	17	10.14	31.24	11.53	10.83	52.36	46.86	
149	M	TIGR	TC158002	na	7/10	Q8LSK6	Homolog to ascorbate peroxidase	<i>L. esculentum</i>	8.65	42.2	6.28	30	17.03	15.11	13.47	14.69	16.99	30.11	
Electron transport																			
52	E	TIGR	TC155238	na	5	Q9LZG0	Similar to adenosine kinase 2	Arabidopsis	5.14	37.8	5.52	40	8.04	9.61	8.00	5.90	4.62	3.55	
44	M	MSDB	S57814	32	12/17	Q9ZSH4	2-Oxoglutarate-dependent dioxygenase	<i>S. chacoense</i>	5.54	37.9	5.98	39	41.25	17.02	10.64	5.80	4.54	0.00	
40	M	MSDB	S01642	33	13/24	P10967	Ripening protein E8	<i>L. esculentum</i>	5.61	41.1	6.1	40	6.77	2.08	5.67	6.72	11.31	11.51	
46	M	MSDB	S01642	40	16/40	P10967	Ripening protein E8	<i>L. esculentum</i>	5.61	41.1	6.12	40	7.37	4.56	5.60	8.15	35.92	40.06	
61	M	MSDB	S01642	13	6/19	P10967	Ripening protein E8	<i>L. esculentum</i>	5.61	41.1	6.23	24	0.00	0.00	0.00	0.00	5.98	9.20	
106	M	MSDB	S01642	36	15/38	P10967	Ripening protein E8	<i>L. esculentum</i>	5.61	41.1	6.09	40	0.00	2.70	6.73	2.01	16.23	19.52	
110	M	MSDB	S01642	37	13/36	P10967	Ripening protein E8	<i>L. esculentum</i>	5.61	41.1	6.21	40	3.00	2.91	1.41	1.58	7.12	13.94	
47	E	TIGR	TC161768	na	4	Q944Z0	Weakly similar to 2-oxoglutarate-dependent dioxygenase	<i>Arabidopsis halleri</i>	5.27	34.0	5.75	37	1.40	1.49	1.08	2.74	7.79	17.36	
Nucleotide metabolism																			
88	M	MSDB	JQ1599	71	10/19	P32518	dUTP pyrophosphatase	<i>L. esculentum</i>	5.19	17.9	5.67	21	17.32	17.57	14.67	11.11	8.39	8.05	
Biogenesis of cellular components																			
111	M	MSDB	O81536	60	21/36	O81536	Annexin P34	<i>L. esculentum</i>	5.38	35.8	5.91	35	12.32	15.31	17.52	13.60	8.61	5.99	
Transport																			
39	M	MSDB	O24345	18	6/10	O82722	Mitochondrial ATPase β -subunit	<i>Nicotiana sylvestris</i>	5.73	59.6	5.67	54	11.02	10.86	11.71	7.77	5.71	3.69	
54	E	TIGR	TC163246	na	6	P32980	Homolog to ATP synthase δ chain	Tobacco	8.96	26.8	5.33	23	5.44	11.99	11.77	14.13	8.85	5.59	
93	M	TIGR	TC163028	37	20/28	Q84XW6	Vacuolar H ⁺ -ATPase A1	<i>L. esculentum</i>	5.2	68.6	5.68	64	5.37	7.77	7.88	6.45	5.34	4.22	
Unclassified																			
139	E	TIGR	TC155857	na	9	At2g37660.1 ⁸	Expressed protein	Arabidopsis	8.37	34.9	6.42	30	15.90	10.67	10.65	8.58	6.62	5.69	
125	E	TIGR	BI927338	na	5	At1g24020 ⁸	Bet v I allergen family protein	Arabidopsis	5.09	17.1	5.52	17	58.47	59.38	37.32	28.13	19.17	12.83	
143	E	TIGR	TC154714	na	16	At3g09350.1 ⁸	Similar to armadillo/ β -catenin repeat family protein	Arabidopsis	5.04	40.4	5.61	50	2.88	6.21	4.18	4.86	6.28	8.09	
117	M	TIGR	TC154018	na	16/30	Q8S4X0	Similar to embryo-abundant protein EMB	Pea	5.44	29.7	6.03	29	4.19	3.56	2.49	1.69	5.67	7.88	

(Table continues on following page.)

Table I. (Continued from previous page.)

Spot No. ^a	MS ^b	Database	Accession No. ^c	Coverage ^d	Peptides Identified ^e	UniProt Accession No.	Assignment	Species	Computed		Observed		Mean % Volume ^f					
									pI	M _r	pI	M _r	7 DPA	14 DPA	21 DPA	30 DPA	Breaker	RR
132	E	TIGR	TC156218	na	3	Q8LF25	Similar to DNA-damage inducible protein DDI1-like	Arabidopsis	4.83	45.4	5.69	42	14.36	32.53	43.09	42.72	44.04	44.54
28	E	TIGR	TC154116	na	12	O82062	Homolog to 39-kD EF-hand containing protein	Potato	4.65	38.9	5.12	42	1.60	2.78	1.87	3.04	5.06	10.94

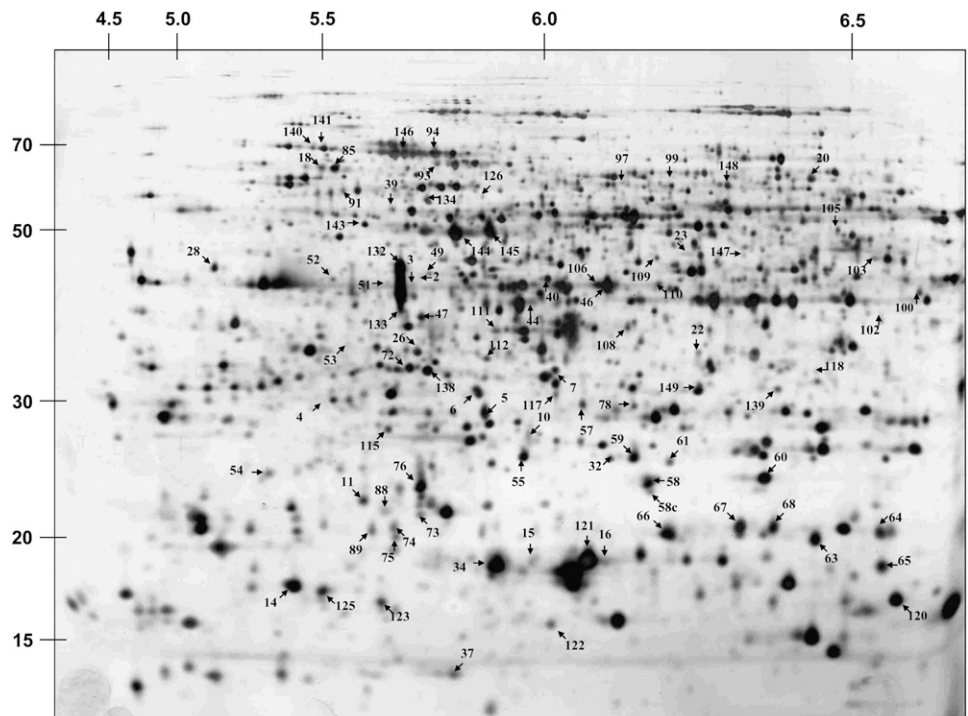
^aSpot number as index in the reference gel. ^bMS method used either MALDI-TOF (M) or LC-MS/MS (E). ^cAccession number of the sequence in the searched database, either MSDB or TIGR EST database. ^dPercent sequence coverage; no available data (na) when EST database was used. ^eRatios indicate number of matching peptides on nonmatching peptides obtained by MALDI-TOF analysis; for MS/MS analysis, the number of identified peptides is given. ^fMean value of the three spot volumes at each analyzed stage. ^gProtein accession number of corresponding sequence in the TAIR database.

acids per sequence ranged from 6 to 24. Among the 90 identified spots, 42 corresponded to tomato sequences (*S. lycopersicum* and *Solanum peruvianum*), 18 to TC that were annotated as related to Solanaceae sequences, 19 to Arabidopsis (*Arabidopsis thaliana*) sequences, and 11 to more phylogenetically distant species. Only two spots corresponded to sequences of unknown function (spots 139 and 143).

When full tomato sequences were available, the experimental M_r corresponded roughly to the theoretical M_r, except for seven spots of β-fructofuranosidase (spots 6, 73, 74, 75, 115, 144, and 145), for the small chain of Rubisco (spot 37), and for lipoxygenase B (spot 148). For all these spots, the experimental M_r was markedly lower than the theoretical M_r. This discrepancy in M_r could be linked either to in vivo or in vitro protein degradation. In vivo, stable breakdown products have been shown to occur, for example, after cold temperatures in rice (*Oryza sativa*) anthers (Imin et al., 2004).

Fourteen proteins were represented by multiple spots with different pI and/or M_r. Thus, the 90 spots actually corresponded to 68 distinct proteins, suggesting that 20% of identified spots corresponded to posttranslational modifications of proteins or were members of multigenic protein families. Figure 4 illustrates some of these spot variations. Most of the multiple spots for a function underwent the same general sense of variation: up- or down-regulation over the course of fruit development (Fig. 4, A–D). In some cases (heat shock protein [HSP] 70, DS2, or S-adenosine methionine [SAM] synthetase), spot intensity showed very similar patterns of variation. In other cases, spots corresponding to the same function were slightly differently regulated. For example, acid invertase (spots 73 and 74) showed the same regulation with marked overexpression at the RR stage, whereas spots 144 and 145 showed a regular increase in spot volume from the 7-DPA to the RR stages. Spot 115 remained slightly

Figure 3. Position of main varying spots on 2-DE silver-stained gel of cherry tomato fruit pericarp at the breaker stage. This gel was used to build the master gel, including 1,791 repeatable spots. It presents the position of the 90 mapped and identified spots annotated in the gel by the number that appears in Table I. Spots that were detected only at other stages than breaker are not visible on this gel.



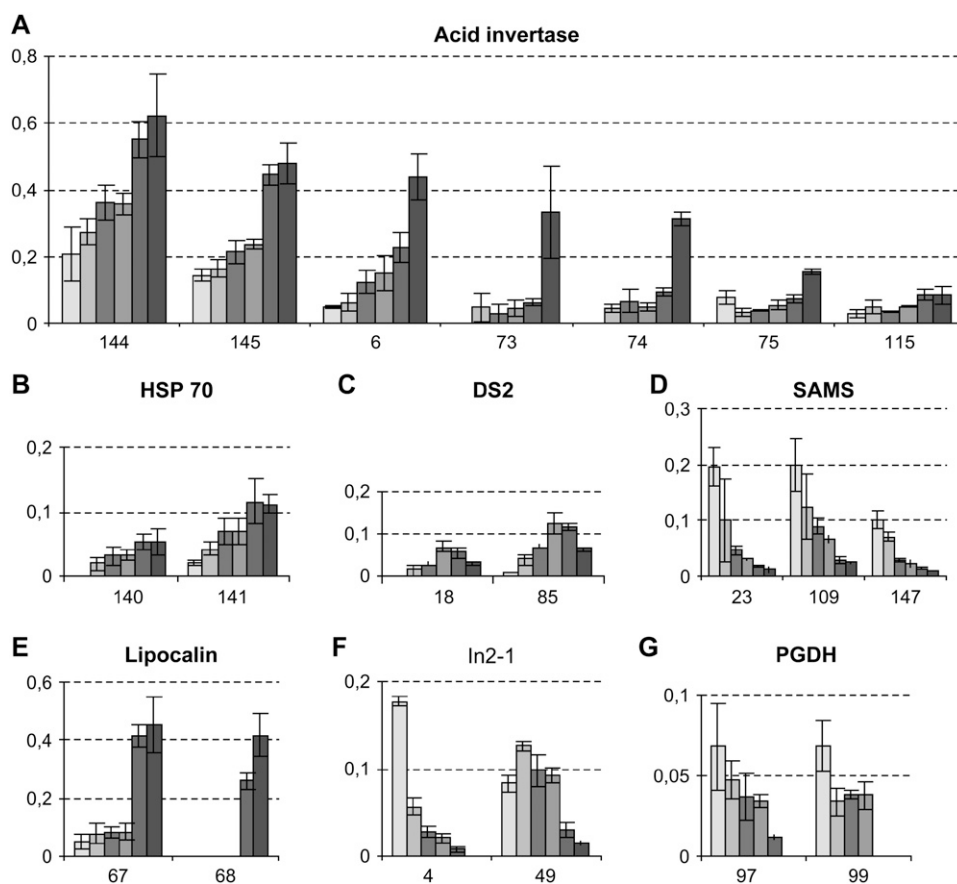


Figure 4. Relative abundance of multiple spots for some proteins during fruit development. The six developmental stages were figured by increasing gray levels. Multiple spots for a protein mainly exhibited the same general sense of variation. In the case of acid invertase (A), up to seven spots were detected showing an increase in spot volume during fruit development. HSP 70 (B) was represented by two spots that underwent an increase in intensity throughout fruit development. The two spots of DS2 protein (C) showed their maximal intensity before ripening. The three spots of SAM synthetase (D) exhibited the same decreasing pattern of variation. In contrast, for lipocalin (E), In2-1 (F), and phosphoglycerate dehydrogenase (G), the two spot isoforms were regulated in a different way.

expressed (Fig. 4A). Regulation of lipocalin or In2-1 showed different patterns, suggesting that the isoforms were implicated in different physiological processes.

Distribution of Spots into Functional Classes

Proteins were categorized by function according to the FunCat scheme (<http://mips.gsf.de>). Distribution of tomato protein spots into putative functional categories is represented in Figure 5. The largest proportion of proteins fell into eight of the 17 categories represented: stress response (21% of spots), C compounds and carbohydrate (17%) and amino acid metabolism (10%), electron transport (9%), photosynthesis and respiration (6%), protein fate, modification, degradation (6%), secondary metabolism (6%), and unclassified (7%). The most striking feature of this classification was the high representation of proteins linked with stress responses, which were mainly up-regulated during the final stages of fruit development. This was also the case for spots linked to C compounds and carbohydrate metabolism or electron transport. In contrast, spots linked to amino acid metabolism were mainly down-regulated, as well as spots related to protein synthesis. Proteins linked to photosynthesis were either down-regulated or transiently increased between 14 and 30 DPA.

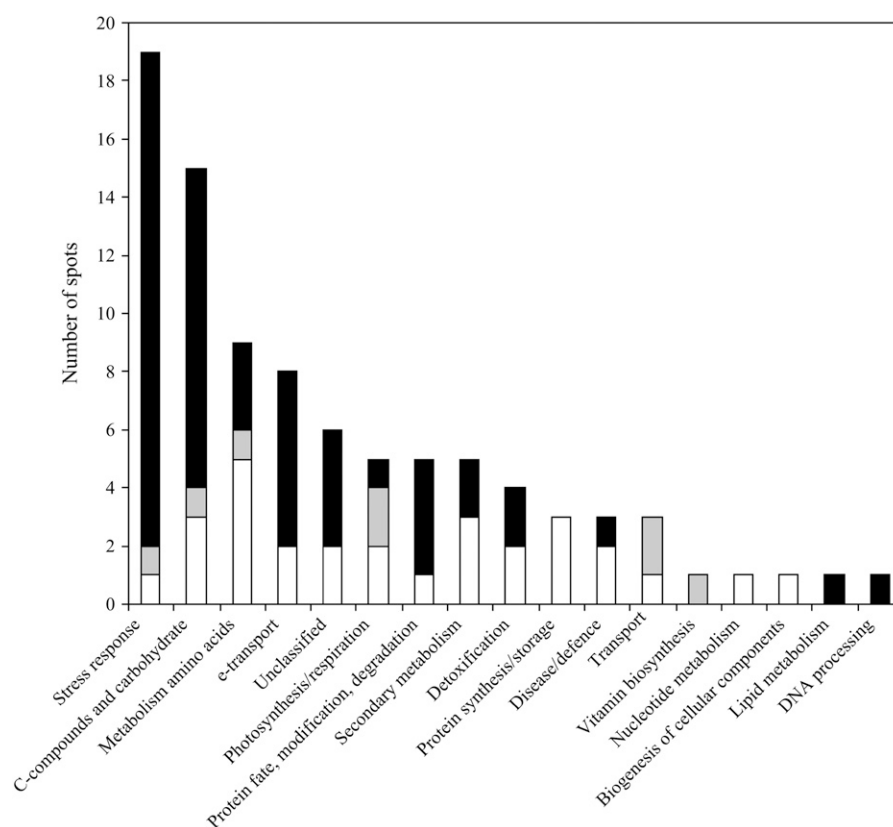
Despite the low number of spots identified for certain functional groups, these spots may also play an essen-

tial role in fruit development. For example, the category nucleotide metabolism was only represented by spot 88, which corresponded to dUTP pyrophosphatase. This enzyme, which ensures the fidelity of DNA replication, has previously been considered to be a good marker of the meristematic state of a cell (Pri-Hadash et al., 1992) in tomato. In our experiment, its variation pattern was in accordance with such a role in fruit growth.

Dynamics of Protein Networks during Fruit Growth and Ripening

To summarize the information contained in Table I and to cluster the proteins showing similar expression profiles during fruit development, hierarchical clustering was applied to the 90 identified spots (Fig. 6A). Spots were classified according to their percentage of volume variations from the 7-DPA to the RR stage using the unweighted pair group method with arithmetic mean (UPGMA). Two main clusters were formed. Cluster I was composed of 36 proteins whose abundance decreased on the whole during fruit development. The first subcluster (from spots 3–16) comprised 15 spots whose maximal quantity was detected at the 7-DPA stage and further decreased until the RR stage. They corresponded to spots mainly expressed during the cell division period. Cluster I also comprised 13 proteins (spots 2–138) whose

Figure 5. Assignment of the identified spots into putative functional categories. Proteins were categorized in 17 classes according to the FunCat scheme (<http://mips.gsf.de>). The distribution of spots overexpressed, underexpressed, or transiently expressed along the tomato fruit growth and development is given for each category. White, Spots whose abundance decreased during fruit development; gray, spots that were transiently expressed; black, spots whose intensity increased on the whole during fruit development.



abundance remained stable during the 7- to 21- or 30-DPA period (i.e. during the overlap of the cell division and cell expansion phases) and then decreased further. Finally, cluster I also comprised eight spots (spots 76–54) whose higher expression took place strictly during the expansion phase (14–30 DPA).

More proteins (54) were clustered in cluster II than in cluster I. Several proteins were specifically induced after ethylene synthesis during the two ripening steps (i.e. the breaker and RR stages). Eleven of them (spots 6–117) showed their higher level of abundance at the RR stage, whereas 29 spots showed a clear increase at the breaker stage and remained stable at the RR stage.

The 13 remaining spots of cluster B displayed varying changes during fruit development and ripening, but with maximal abundance at the RR stage.

As shown by the transposed cluster tree (Fig. 6B), the phase effect was the main factor explaining spot variations. The six samples clustered into three subtrees, corresponding to cell division (7 and 14 DPA), cell expansion (21 and 30 DPA), and fruit maturation phases (breaker and RR stages).

DISCUSSION

2-DE-Based Proteomic Approach to Reexamine Tomato Fruit Development

Despite the increasing interest in plant proteomics (Cánovas et al., 2004), very few results have been

published on tomato proteomics and, especially, on the tomato fruit proteome. Apart from technical articles (Saravanan and Rose, 2004), published data concern the proteome of developing tomato seeds (Sheoran et al., 2005), the impact of heat stress on fruit protein expression (Iwahashi and Hosoda, 2000), or the effect of a physiological disorder (blossom-end rot) on the fruit proteome (Casado-Vela et al., 2005). Recently, fruit proteins of two tomato ecotypes were compared (Rocco et al., 2006). This work aims to precisely correlate protein variations with fruit growth and ripening.

Protein Variations as Compared to Transcriptomic and Metabolomic Data

Among the 1,791 spots of the master gel, 148 spots (about 8%) were found variable in intensity throughout the process of fruit development. This represents a slightly lower percentage than that detected by transcriptomic analysis (Alba et al., 2005), where 10% of genes were differentially expressed in developing tomato pericarp. The majority of proteins that have been characterized here correspond to genes known to be regulated during tomato fruit development. Most of them display temporal expression consistent with the succession of different phases of fruit development. Previously, tomato fruit digital analysis (Fei et al., 2004) detected 518 ripening-related genes when comparing mature green to breaker fruit, with more genes up-regulated (333) than down-regulated (185).

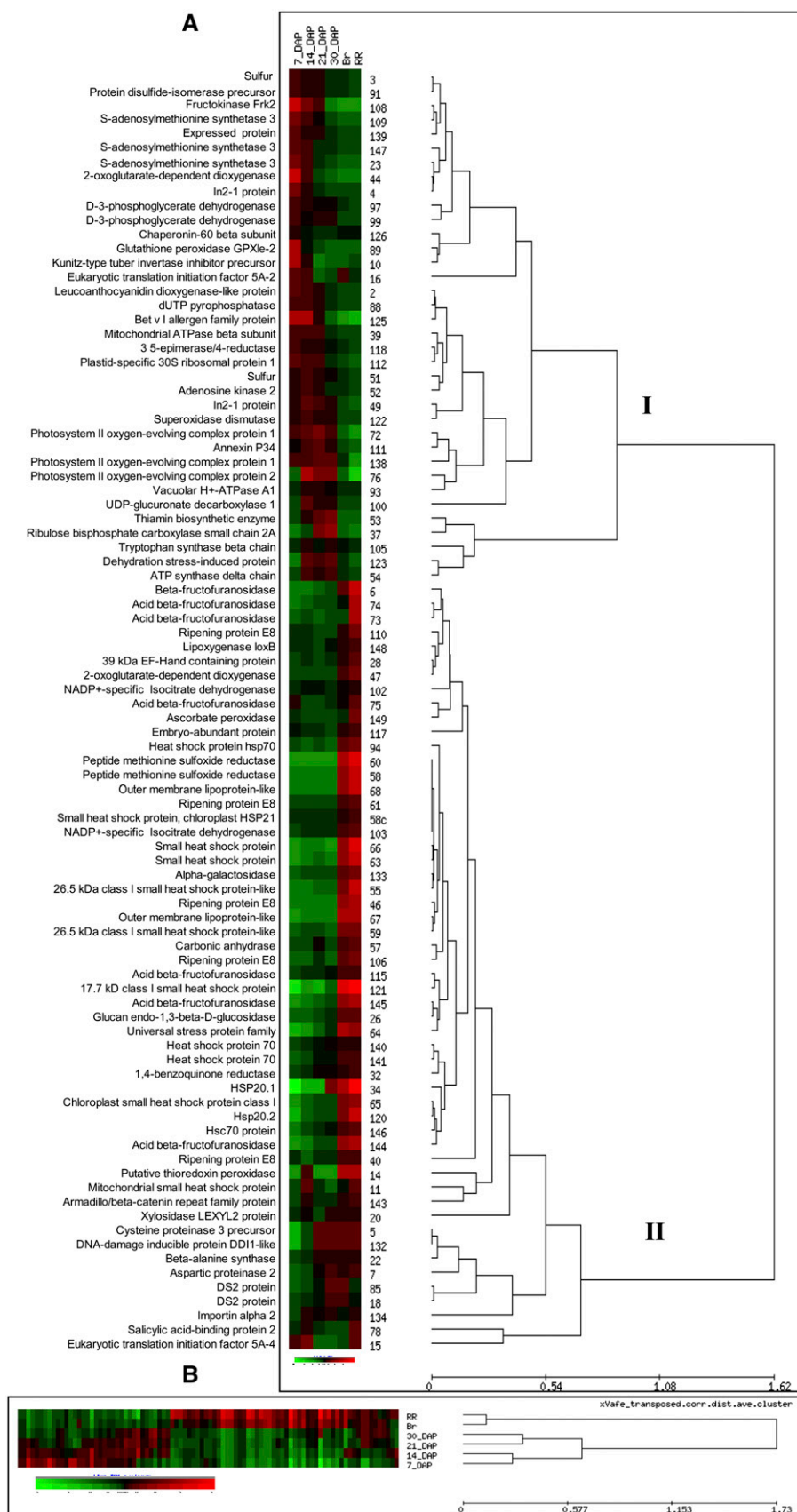


Figure 6. Hierarchical clustering analysis of the 90 identified spots. A, Spots listed in Table I were clustered according to their percentage of volume from 7 DPA to the RR stage using the UPGMA method. The spot number is indicated on the right of the heat plot; the functional annotation is on the left side. Cluster I was composed of 36 protein spots whose abundance decreased on the whole during fruit development. Cluster II grouped together 54 spots overexpressed during the last stages of fruit development. B, Clustering of studied fruit growth stages (7 DPA to the RR stage). The six stages of development clustered in three groups, corresponding to cell division (until 14 DPA), cell expansion (until 30 DPA), and fruit ripening phases.

We also found more up-regulated than down-regulated spots (54 versus 36), but a certain discrepancy exists between our proteomic data and available digital analysis data. For some functions, fruit ESTs were not present in TIGR database (e.g. spots 20, 63, 123, 54, 88, and 132). Otherwise, spot and EST variations between these two developmental stages were mainly identical. Our work is complementary to that of Alba et al. (2005): Transcriptome profiling via cDNA TOM1 microarrays allowed identification of 869 genes that were differentially regulated during nine stages of tomato fruit development. Among them, 72 shared homology with signal transduction or transcription factors. A global proteomic approach does not give access to weakly expressed proteins and a specific experimental design would be required to study nuclear proteins. However, it is important to note that, among the 90 identified varying spots in our study, 15 corresponded to 13 gene sequences that do not figure on the TOM1 microarray (spots 2, 4, 10, 22, 26, 34, 47, 49, 63, 66, 78, 105, 123, 125, and 134). They represented 16.5% of the gene sequences identified in this work. Moreover, 36 varying spots corresponded to sequences on TOM1, but not mentioned as variable by Alba et al. (2005). Finally, when similar functions were addressed (31 spots), different patterns of expression were sometimes noticed. In the same way, our results sometimes showed differences with electronic northern data given by TIGR database. Some differences could be linked to the studied genotypes or to the number of developmental stages. However, the differences also point out the relevance of a proteomic approach. When compared with the RNA level, the protein level integrates posttranscriptional and translational processing that modulates the quantity, temporal expression, localization, and efficiency of the final product in the cell. We could, indeed, identify some protein modifications in the form of multiple spots (Fig. 4). Part of them showed slightly different patterns of expression (e.g. lipocalin, In2-1, or sulfur), suggesting regulation mechanisms and possibly different effects in tomato fruit. As a matter of fact, some recent results have shown the impact of a posttranslational mechanism in metabolic regulation during tomato fruit development (Carrari et al., 2006).

Some of the protein functions that we identified in this study are well known in the scientific context of fruit development and maturation. We will thus emphasize in the following discussion the proteins for which our results bring new insights.

Proteomic Patterns Are Associated with the Physiological Stages of Fruit during Development

Cervil fruit growth exhibited a classical sigmoid pattern either when measured in fresh weight or in fruit diameter. Cell number and volumes were consistent with previously published results (Gillaspy et al., 1993; Joubès et al., 1999). In its early stages, fruit growth was primarily the result of cell divisions, but

when cell divisions ceased, fruit growth continued by cell expansion. In Cervil, a small fruited genotype, cell division had almost stopped when cell expansion took place. Previous results showed that this behavior differs from that of a large fruited tomato, Raïssa, which was shown to divide until 20 to 25 DPA, whereas cell expansion started from 15 DPA (Bertin et al., 2003; Bertin, 2005). Our results confirmed that increase in pericarp cell size occurred while fruit weight increased (Cheniclet et al., 2005). The chosen stages for proteomic studies corresponded either to characteristic times of each phase of development (7, 21, RR, respectively, for cell division, cell expansion, and fruit ripening) or to overlapping periods (14, 30, and breaker, respectively, for the end of cell division, the end of cell expansion, and the beginning of fruit coloring). Regarding variations of spot abundance, clustering of the 90 protein spots clearly showed that the phase effect is the main factor explaining spot variations (Fig. 5B). Indeed, the six samples clustered into three subtrees corresponding to division (7 and 14 DPA), expansion (21 and 30 DPA), and maturation phases (breaker and RR stages). Variations in the fruit proteome pick out the main physiological stages of fruit development and some of the detected proteins may play a role in the related processes. The result is to bring together, with the clear distinction of tomato fruit, developmental stages previously obtained by metabolome profiling (Roessner-Tunali et al., 2003).

Based on these stages of development, we could identify functional categories of spots that are up- or down-regulated during fruit development (Fig. 5). Spots linked to metabolism (24 for C compounds and carbohydrate and amino acid metabolism) represented the largest class, being mainly up-regulated for carbohydrate metabolism and down-regulated for amino acid metabolism. As previously noted (Fei et al., 2004), another important class was genes related to stress response (19 members). Ripening is marked by oxidative processes and HSP, at least chaperones, could play a role in stabilizing proteins. In tomato, small HSPs have already been shown to be involved in fruit developmental processes (Lawrence et al., 1997; Löw et al., 2000; Neta-Sharir et al., 2005). Finally, some signature proteins can be proposed to characterize stages of development. For example, no spot could be detected for HSP21 (TOM111) or protein E4 until the breaker stage. On the other hand, a thiamine biosynthetic enzyme spot was detected from 7 to 30 DPA, but was no longer present at the breaker and RR stage. This enzyme was shown to be specifically expressed in the tomato outer pericarp cell layers at 22 DPA (Lemaire-Chamley et al., 2005). Signature proteins might be of great interest to compare genotypes exhibiting different fruit growth kinetics.

In contrast, some spots showed a biphasic pattern of regulation. Spots 16, 14, 11, 143, 78, and 15 were over-expressed both during cell division and maturation, suggesting either that these proteins could be involved in different physiological processes or that the same

physiological process could take place at different phases of fruit development.

Proteomic Survey of Early Stages of Fruit Development in Tomato Pericarp

Young tomato fruit were characterized by higher protein content than ripe fruit, confirming that protein content in fruit decreases during development (Jimenez et al., 2002; Andrews et al., 2004). Proteins highly expressed in young fruit were mainly addressed to the cytoplasm or the chloroplast and were linked with primary metabolism (either sugar or protein metabolism), photosynthesis, oxygen radical scavenging, and cell wall metabolism. Besides proteins linked to young fruit metabolism, our study identified some proteins whose expression is related to cell division or cell expansion and might be implicated in increase in size of young fruit.

Young Fruit Metabolism

Green tomatoes contain photosynthetically active chloroplasts that could contribute between 10% and 15% of the carbon skeletons in green fruits (Tanaka et al., 1974). Several spots linked with photosynthesis were overexpressed in young tomato fruit. Three spots of PSII (72 and 138 for protein 1, 76 for protein 2) and protein 1 from the plastid ribosomal 30 S subunit (spot 112) were also overexpressed during this period. Spot 37 was related to Rubisco small chain 2A, but its observed molecular mass was lower than expected (7 instead of 20.3). It might correspond to a degradation product from the Rubisco small chain. Sulfur (spots 3 and 51) is a subunit of magnesium chelatase, which is responsible for the first step in chlorophyll synthesis (Reid and Hunter, 2002). Its activity is coordinated with plastid biogenesis and it possesses high regulatory properties (Papenbrock and Grimm, 2001). The gradual decrease of photosynthesis-related protein abundance is an established observation (Rocco et al., 2006) and is associated with the transition from chloroplast to chromoplast. Carrari et al. (2006) also reported a tendency of transcript levels of photosynthesis genes and metabolically associated genes to be reduced during fruit development. The observed high expression of chaperonin 60 (spot 126) at an early stage of fruit development, followed by a regular decrease, was consistent with electronic northern data. This plastid chaperonin may be implicated in protein folding, in particular in Rubisco assembly (Vierling, 1991). Moreover, another protein implicated in protein folding was accumulated during the cell division phase: protein disulfide isomerase (spot 91), which facilitates folding through its ability to reduce or oxidize disulfide bridges in the presence of a reducing or an oxidizing agent (Gilbert, 1997).

The thiamine biosynthetic enzyme (spot 53) is another chloroplastic protein. It is an essential cofactor required for the activity of enzymes associated with

major metabolic pathways. In tobacco (*Nicotiana tabacum*), a thiamine-deficient mutant did not produce chlorophyll and carotenoids (McHale et al., 1988). However, in citrus, it was shown to be involved in fruit maturation (Jacob-Wilk et al., 1997); this is contradictory to our results on Cervil tomato, where it appeared to be strictly related to young green fruit.

Concerning sugar metabolism, two proteins exhibited noteworthy variations. Frk2 was one of the most intense protein spots (108) at 7 DPA. It is the major fructokinase in tomato fruits; its contribution to Fru phosphorylation activity is known to be very significant. In the past, it was supposed to be implicated in starch accumulation, but fructokinase antisense plants are able to accumulate starch. It has been suggested that it may play a role in sugar import rather than starch biosynthesis (Dai et al., 2002). The proteomic pattern of Frk2 was consistent with digital analysis results. Also concerning sugar metabolism, spot 10 was predominantly expressed at 7 DPA. It was identified as a putative Kunitz-type invertase inhibitor. No electronic northern expression data are available on this sequence, but the observed proteomic variation could be inversely correlated with acid β -fructofuranosidase (spots 6, 57, 73, 74, 75, 115, 144, and 145) expression, which reaches a maximum during the maturation period. The Kunitz-type invertase inhibitor plays a role in plant defense mechanisms against pests and diseases, but, recently, a Kunitz-type inhibitor from potato (*Solanum tuberosum*) tuber was found to inhibit soluble invertase (Glaczinski et al., 2002). Its role in sugar metabolism in tomato fruit might deserve more in-depth investigation.

Concerning amino acid metabolism, two proteins were overexpressed during early tomato development: the β -chain of Trp synthetase (spot 105), which catalyzes the final step of Trp biosynthesis and D-3-phosphoglycerate dehydrogenase (spots 97 and 99), which is implicated in Ser biosynthesis through the 3-phosphoglycerate pathway. This last protein is supposed to supply Ser in nonphotosynthetic tissues and in tissues undergoing rapid cell proliferation (Ho and Saito, 2001). The three spots underwent similar volume variations compatible with TIGR EST expression data. It is unclear whether expression of the spots of SAM synthetase 3 (spots 23, 109, 147) is strictly related to the regulation of Thr and Met accumulation. This enzyme catalyzes the biosynthesis of S-adenosyl-L-Met (AdoMet), which represents the major methyl group donor for several biological transmethylation reactions. AdoMet is involved in a variety of cellular processes; notably, it is a precursor of ethylene synthesis and of the phenylpropanoid constituents of the cell wall. Its expression might be induced during cell wall synthesis or modification (Espartero et al., 1994).

Increase in Size of Young Fruit

Some of the detected spots corresponded to proteins putatively involved in cell division or cell wall

expansion. For example, eukaryotic initiation factor (eIF)-5A is an interesting case of two spots corresponding, respectively, to isoforms 5A2 (spot 16) and 5A4 (spot 15). These spots showed two peaks of expression: during division, but also at the ripening stage, eIF-5A4 being more intense overall than eIF-5A2. Their expression patterns showed a slight time lag; the eIF-5A2 spot volume was maximal at 7 DPA and the breaker stage, whereas the eIF-5A4 spot volume was maximal at 14 DPA and the RR stage. These patterns of variation are in accordance with eIF-5A function. eIF-5A does not act as a conventional translation initiation factor because it seems not to be required for global protein synthesis, but appears to function as a nucleocytoplasmic shuttle protein. It is known to be activated post-translationally by modification of Lys into the unusual amino acid hypusine and is supposed to play a determinant role in the translation of mRNAs required either for cell division or cell death (Thompson et al., 2004). In tomato, 5A2 and 5A4 were previously associated with senescing fruit and programmed cell death (Wang et al., 2005). Our results seem to confirm that they also may play a role, during the cell division process, as previously demonstrated in yeast (*Saccharomyces cerevisiae*; Park et al., 1998). Also overexpressed during young fruit development was a protein that has been previously considered to be a good marker of the meristematic cell state in tomato (Pri-Hadash et al., 1992). dUTP pyrophosphatase (spot 88) hydrolyzes dUTP to dUMP and pyrophosphate. Because it decreases the intracellular concentration of dUTP, uracil cannot be incorporated into DNA and the fidelity of DNA replication and repair is ensured.

A puzzling observation is the variation pattern of spot 134, importin α , which is a nuclear shuttle protein. It increased between 7 and 14 DPA, where it reached its maximal quantity and remained unchanged until the RR stage. Because it has been shown to interact with the cytoskeleton, it is supposed that it could inactivate spindle formation during mitosis (Gruss et al., 2001). Deeper investigation would be required to confirm such a role in the cell cycle in young tomato fruit.

In plants, it is well established that the cell cycle is controlled by the redox status, oxidative stress leading to cell cycle arrest (Reichheld et al., 1999). Reactive oxygen species are produced by photoreduction of O_2 during photosynthesis. Young Cervil fruit expressed some spots linked to oxidative stress, high levels of glutathione peroxidase (GPX1e-2), and superoxide dismutase (SOD). Moreover, two spots of In2-1 protein (spots 4 and 49), which shows similarity to potato pathogenesis-related protein 1 and presents a glutathione S-transferase domain, are overexpressed during the initial stages of fruit development with a slightly different regulation feature (Fig. 4). All these proteins presented their maximal spot intensity at 7 or 14 DPA. These results are in accordance with those of Wang and Jiao (2001) on blackberry (*Rubus fruticosus*) fruit. Moreover, SOD

activity fits better with our proteomic results than with mRNA expression (Jimenez et al., 2002). The SOD spot we identified is a more acidic one than the spot identified by Rocco et al. (2006), which is also present on our gels, but did not show significant abundance variation in Cervil. This explains our divergent results on SOD variations.

After the intensive division period, fruit enlarges almost solely by cell expansion, which requires cell wall elongation and accumulation of solutes within the vacuole. Vacuolar H^+ -ATPase is a multimeric enzyme that contributes to the generation of the proton gradients across the tonoplast. Antisense suppression of this enzyme reduces fruit growth, but does not affect sugar concentration in tomato fruit (Amemiya et al., 2006). It is supposed that V-ATPase is necessary for vacuolar acidification and for sorting of soluble proteins as vacuolar invertase. It can also promote cell growth by playing a role in membrane fusion events and exocytosis of wall material. Our results showed that the expression of H^+ -ATPase 1 was actually enhanced during the cell enlargement phase. Annexins are also potentially involved in cell expansion and exocytosis. Annexins are a large family of multifunctional proteins that bind phospholipids in a calcium-dependent manner. Among the different roles suggested for these proteins is their involvement in Golgi-mediated secretion of polysaccharides (Clark et al., 2001). In tobacco, annexin P34 is supposed to participate in the vacuolation process of expanding cells (Seals and Randall, 1997). Our results showed that tomato annexin P34 expression was well correlated with cell expansion as it increased from 7 to 21 DPA and then decreased. In strawberry (*Fragaria* spp.) and pepper (*Capsicum annuum*), a slightly different pattern of expression was reported: annexin expression increased during development until fruit maturation (Wilkinson et al., 1995; Proust et al., 1996). Based on electronic northern data, no noticeable variation in the annexin P34 gene occurred during fruit development. As a matter of fact, some other proteins overexpressed during the cell expansion period could also be linked to cell wall metabolism. In Arabidopsis, a 3,5-epimerase/4-reductase (spot 118) is involved in synthesis of L-Fuc or L-Rha, which are precursors of the cell wall pectic polysaccharides rhamnogalacturonan I and II. Because Solanaceous species contain little, if any, Fuc, this enzyme may act as a Rha synthase as previously described (Watt et al., 2004). UDP-glucuronate decarboxylase 1 (spot 100) showed an increase in intensity during the cell elongation phase. This protein is implicated in Xyl synthesis and was shown to be highly expressed in Arabidopsis cells during cell wall synthesis (Molhoj et al., 2003). Finally, adenosine kinase 2 (spot 52) is implicated in transmethylation activity and regeneration of SAM (Weretilnyk et al., 2001). There is a direct correlation between adenosine kinase activity and the level of methylesterified pectin in Arabidopsis seed mucilage (Moffatt et al., 2002).

Proteomic Survey of Molecular Mechanisms Occurring during the Ripening Stage in Tomato Pericarp

Fruit ripening is a complex, well-documented, but not yet fully elucidated, phenomenon (Giovannoni, 2001). Major physiological modifications that affect color, texture, flavor, and aroma are under the control of both external (light, temperature) and internal (developmental gene regulation, hormonal control) factors. At the cellular level, several biochemical pathways are redirected, leading to substantial modifications of the RR tomato proteomic pattern in regard to the young fruit pattern (Fig. 2). Also among proteins overexpressed at the ripening stage were some proteins whose expression was already increasing during the expansion stage (Fig. 6A). Among the 54 spots of cluster II were mainly proteins related to fruit maturation, cell wall modifications, stress response, and senescence. Most of these proteins are cytoplasmic and vacuolar and some of them are secreted. Only a few nuclear-encoded small HSPs were found to be addressed to the chloroplast/chromoplast using TargetP software. Proteins overexpressed at maturation stages were mainly linked to ripening processes, but many of them were related to stress responses and fruit senescence.

Ripening Processes

The two main proteins overexpressed in ripening tomato were β -fructofuranosidase (acid invertase) and protein E8, each of them being well known as ripening-induced functions. They showed, respectively, seven and five different spots that represented about 3% and 1% of the total image gray level from the 1,730 spots detected at the RR stage. Our results showed that acid invertase corresponded to seven spots exhibiting different M_r and variation patterns. Acid invertase catalyzes hydrolysis of Suc into Glc and Fru. EST expression data showed that the gene was mainly expressed at the breaker stage; however, our results showed that a shift in expression existed at the protein level, the highest spot intensity being obtained at the RR stage. The increase in acid invertase enzyme activity during fruit maturation and ripening and the fragmentation of the protein into several polypeptides during plant development have been previously reported (Sturm, 1999). On our 2-DE gels, acid invertase molecular mass varied from 20 to 49 kD, whereas the molecular mass of the precursor protein is about 70 kD. Expression patterns of spots 144, 145, and 6 showed a gradual increase, whereas spots 73 and 74 were mainly expressed at the RR stage (Fig. 4). The physiological significance of developmental regulation of these polypeptides remains to be explored.

The function of E8 proteins is still unknown, but they share extensive sequence similarity with numerous oxidoreductases and are known to be expressed during fruit ripening. E8 proteins are regulated by ethylene during tomato fruit ripening and have been

shown to exert a negative effect on ethylene biosynthesis (Penarrubia et al., 1992). E8 proteins belong to a multigenic family that has been shown to include more members in tomato than in Arabidopsis. The expansion of this gene family in tomato suggests an important adaptation for fruit ripening (Van der Hoeven et al., 2002). In our experiment, five spots corresponded to the same accession of E8, four of them (except spot 61) having a M_r of 40, compatible with theoretical M_r , and being expressed even at earlier stages of fruit development, but with a strong increase from the breaker stage, confirming electronic northern data. According to its M_r (24), spot 61 could correspond to a degradation product. This spot was, however, present in another tomato genotype, where it exhibited the same variation pattern during fruit growth (data not shown). The physiological impact of differential regulation of the different spots of acid invertase and E8 protein has to be explored.

The protein extraction method used was not devoted to cell wall protein characterization. This is one of the reasons why we only showed the presence of a few cell wall hydrolases. Among them, a hemicellulase, β -xylosidase (LeXyl2), increased during cell expansion and remained constant during fruit maturation. Such variation is similar to previous results (Itai et al., 2003). However, no EST related to LeXYL2 was present in tomato fruit EST databases. It is widely assumed that β -galactosidase plays an important role in tomato ripening because cell walls of ripening fruit undergo a loss of galactosyl residues from cell wall polymers (Brummell and Harpster, 2001). However, on our 2-DE gels, another exoglycosidase, α -galactosidase, could be identified from a spot showing marked intensity increase at the breaker and RR stages. α -Galactosidase is capable of hydrolyzing α -1,6 linked α -galactoside residues and α -galactosidase activity was shown to increase substantially during ripening in fruits, among them papaya (*Carica papaya*), grape (*Vitis vinifera*), and tomato (Kang and Lee, 2001; Jagadeesh et al., 2004; Owino et al., 2005; Soh et al., 2006).

β -1,3-Endoglucanases are ubiquitous enzymes in plants that hydrolyze 1,3- β -D-glucosidic linkages in 1,3- β -D-glucans to release Glc monomers. Besides their well-known role in defense mechanisms against fungal attack, there is strong evidence that these enzymes are involved in non-defense-associated processes like cell division, pollen development, seed germination, bud dormancy, and fruit ripening (Peumans et al., 2000). In tomato, spot 26 showed a marked increase between 30 DPA and the breaker stage, addressing the question of its possible involvement in the ripening process in tomato insofar as no pest or disease could be noted on our plants.

Stress Responses and Fruit Senescence

During ripening, a major part of the proteomic response was related to stress and senescence (Fig. 5),

supporting the idea that fruit ripening is accompanied by an important oxidative process. In tomato, hydrogen peroxide accumulates at the breaker stage (Jimenez et al., 2002) when chloroplasts differentiate in chromoplasts. This transition requires massive transformation of the plastid internal membrane structure as the photosynthetic apparatus is disassembled. We identified two chloroplastic antioxidant proteins. Ascorbate peroxidase (spot 149) represents the most important hydrogen peroxide-scavenging enzyme in plants. In our experiment, ascorbate peroxidase showed a constant level of expression from 7 DPA to the breaker stage, but a marked increase at the RR stage. Such an expression pattern is quite consistent with the previous results of Rocco et al. (2006) and with enzyme activity (Jimenez et al., 2002), but slightly divergent from mRNA expression. The second enzyme was a putative thioredoxin peroxidase (spot 14). This enzyme is less efficient than ascorbate peroxidase and is regenerated via thioredoxin. As far as we know, no data are published yet on the role of this protein in fruit ripening. The spot pattern of expression showed a bimodal curve, the enzyme being overexpressed at 14 DPA and the breaker and RR stages. Oxidative stress also causes protein oxidation and lipid peroxidation. The overexpression of peptide Met sulfoxide reductase (E4; spots 58 and 60) after ethylene induction during ripening is, on the other hand, well documented in tomato and strawberry fruit (Lincoln et al., 1987; Lopez et al., 2006). This protein is implicated in repair of oxidized damaged proteins. Its spot expression was strictly linked with the breaker and RR stages. Concerning lipid peroxidation, we actually observed an increase of lipoxygenase B (spot 148) as fruit grew and ripened. TomLoxB is one of the five isoforms of lipoxygenase of tomato and it is fruit specific. It is not involved in flavor volatile production, but its expression is enhanced by ethylene (Chen et al., 2004). We also identified two spots of outer membrane lipoprotein-like protein exhibiting highly different patterns, suggesting a posttranslational regulation phenomenon (Fig. 5) and possibly different roles for the two spots. The first lipocalin-like proteins reported in plants were the two enzymes violaxanthin deepoxidase and zeaxanthin epoxidase, which catalyze the interconversion between the carotenoids violaxanthin, antheraxanthin, and zeaxanthin, playing a role in the xanthophyll cycle and the protection against photooxidative damage (Hieber et al., 2000). Enhancement of these compounds in tomato fruit during ripening was recently measured (Carrari et al., 2006).

Although they were first described as induced by heat stress, HSPs are overexpressed under several types of stress and also during plant development. They are well known for their roles in the maturation of protein complexes and degradation of damaged or misfolded peptides, and for regulating the activity of many signal transduction proteins. Our study picked out 14 up-regulated HSP spots during fruit development and ripening. They were highly coregulated, as

demonstrated by their closed positions into the same cluster branch. Four of them corresponded to sequences of HSP 70 molecular chaperones (spots 94, 140, 141, and 146). In tomato, HSP 70 has been shown to be developmentally regulated (Duck et al., 1989). According to TIGR EST database, they were expressed at the breaker stage. Their role during fruit ripening is probably linked to the prevention of protein aggregation, facilitation of the renaturation of aggregated proteins during the oxidative stress encompassed by the fruit. The same role has also been suggested for small HSPs (Sun et al., 2002). In our study, among the 10 small HSP spots, the majority showed a regular increase in spot intensity throughout fruit development. They were mainly distributed to the chloroplast/chromoplast (spots 34, 120, 65, 58c, and 121) or to the mitochondria (spots 11, 55, and 59) and two were addressed to the secretion pathway (spots 63 and 66). Particularly striking is the accumulation pattern of spot 34 corresponding to HSP 20.1, whose total spot volume at the RR stage was the greatest of all the studied spots and corresponded to 10-fold accumulation. Neta-Sharir et al. (2005) showed that tomato HSP 21 (spot 58c) protects PSII from temperature-dependent oxidative stress, but also promotes carotenoid accumulation in developing fruit. Moreover, another tomato small HSP (*vis1*) is known to play a role in pectin depolymerization during ripening, determining viscosity attributes of tomato fruit juice (Ramakrishna et al., 2003). On top of these stress-related proteins, spot 64 was identified as similar to a universal stress protein from *Arabidopsis* related to ER6, which is induced by ethylene during ripening (Zegzouti et al., 1999). Corresponding electronic northern data were in accordance with spot variation. In rice, it is supposed to play a role in ethylene-mediated stress adaptation (Sauter et al., 2002). Apart from antioxidant proteins, some proteins related to dehydration stress were overexpressed during ripening, suggesting an effect of environmental conditions in the greenhouse during fruit ripening. Spot 123 corresponded to a TC weakly similar to a dehydration stress protein-induced protein and spots 18 and 85 were identified as the DS2 protein, which is a protein homologous to abscisic acid, stress, and ripening-induced protein and supposed to play a role in osmotic protection.

Several proteinases, including Cys proteinase or aspartic proteinase, participate in programmed cell death and stress responses. Spot 5 corresponded to SENU3, a Cys proteinase. It was formerly reported to be expressed during senescence of tomato leaves and in fruits, whereas its mRNA expression decreases as fruit start ripening (Drake et al., 1996). At the protein level, we could observe a regular increase of this spot intensity until the RR stage. A similar pattern of variation was recorded for an aspartic proteinase (spot 7).

Our results pointed out two spots (102 and 103) corresponding to a cytosolic NADP⁺-specific isocitrate dehydrogenase whose intensity increased during fruit development and ripening, confirming previous

observations (Gallardo et al., 1995). This enzyme catalyzes the conversion of isocitrate to 2-oxoglutarate, which is the metabolic signal that regulates coordination of carbon-nitrogen metabolism (Galvez et al., 1999). It could be implicated in ammonia reassimilation during senescence or in Glu accumulation contributing to ripe tomato flavor. It might be important to make a link between this protein and spot 47, which corresponds to a 2-oxoglutarate-dependent dioxygenase and exhibits a similar pattern of variation with a potential role in biosynthesis of hormone or secondary metabolites.

CONCLUSION

This article provides an overview of the main cherry tomato proteome variations during precise stages of fruit growth and ripening. 2-DE profiles showed variations in some spots' relative abundance. All spots submitted to MS analysis were identified. About one-third of varying protein spots were overexpressed during the early stages of fruit development and their expression decreased during fruit maturation, the remaining spots being overexpressed during the ripening stages. In some cases, the spot pattern of expression and the spot function argue for a role in major fruit physiological developmental processes. Some spots could then be related to fruit increase in size by their role in either cell division or cell expansion. Some other spots could be related to fruit maturation. They were mainly involved in ripening processes, but also to stress responses and fruit senescence. When comparing our results with those of previously published transcriptomic studies, some discrepancies were noted, confirming the necessity to carry on proteomic analysis and to go deeper in the analysis of functional meaning of protein posttranscriptional and translational modifications. This point is also underscored by recent data in the metabolome-profiling area.

MATERIALS AND METHODS

Plant Material and Biological Measurements

Plants of tomato (*Solanum lycopersicum* var. *cerasiforme*; Cervil) were cultivated in a greenhouse in a full randomized trial. Temperature conditions in the greenhouse were 16°C during the night and 20°C during the day. Inflorescences were pollinated with an electrical shaker and the date of anthesis of each individual flower was recorded.

The fruit diameter was measured on fruits at different positions within the inflorescence, twice and then once a week to assess fruit growth in a nondestructive manner. Pericarp cell number was measured on fruits at different positions on the third inflorescence of 10 plants. Fruits were collected at different ages: from anthesis to 12 DPA, around 20 DPA, and during maturity (from 39–44 DPA). Cell suspensions were obtained after maceration of the pericarp in a pectinase solution (Bünger-Kibler and Bangerth, 1982; Bertin et al., 2002) containing 3.5% (w/v) pectinase (Fluka), 0.1 M EDTA, and 0.4 M mannitol. Cells of an aliquot of the suspension were counted under a microscope using counting chambers (Fuchs-Rosenthal chamber, 0.2-mm depth for

large fruits, and Burkner chamber, 0.1-mm depth for small fruits). A minimum of eight samples per fruit was counted. The total number of cells in the whole fruit pericarp was calculated from volumes of the counting chamber, maceration solution, and pericarp.

The mean cell volume was calculated by dividing the pericarp volume (measured by water displacement) by the total number of pericarp cells. Measurements of cell area made in situ on pericarp slices showed that this ratio is a good indicator of cell size, considering that the total intercellular space of tomato pericarp is relatively reduced (N. Bertin, unpublished data).

For proteomic analysis, fruits were harvested at the following six stages of development: 7, 14, and 21 DPA, defined as immature green, 30 DPA, defined as mature green, breaker (when the fruit starts to turn from green to orange), and RR (5 d after orange stage). Special care was taken to harvest fruits of different stages on the same day; thus protein variation along fruit development could not be attributed to climatic condition changes. Pericarps were collected from at least 15 different fruits, immediately frozen in liquid nitrogen, and stored at -80°C prior to grinding into a fine powder in prechilled steel cylinders by a mixer mill.

Preparation of Total Protein Extracts

For each stage of development, three independent protein extractions were performed as previously described (Faurobert et al., 2006). Plant powder was suspended in 3 volumes of extraction buffer (containing 700 mM saccharose, 500 mM Tris, pH 8, 100 mM KCl, 2% [v/v] β -mercaptoethanol, 2 mM phenylmethylsulfonyl fluoride, pH 8.5) and incubated for 10 min on ice. Afterward, an equal volume of Tris-saturated phenol was added. Samples were shaken for 10 min at room temperature and then centrifuged (10 min, 5,525g, 4°C) to separate the phenolic and the aqueous phase. The phenolic phase was recovered and reextracted with the same volume of extraction buffer. Subsequently, centrifugation was repeated and 5 volumes of precipitation solution (0.1 M ammonium acetate in methanol) were added to the recovered phenol phase. Proteins were allowed to precipitate at -20°C overnight. After centrifugation for 10 min (5,525g, 4°C), the protein pellet was washed three times with the precipitation solution and once with acetone. Each washing step was followed by 5 min of centrifugation as described above.

After drying under vacuum, the pellet was resuspended in lysis buffer (9 M urea, 4% [w/v] CHAPS, 0.5% [v/v] Triton X-100, 20 mM dithiothreitol [DTT], 1.2% [v/v] pharmlalyte, pH 3–10) and protein concentration was measured according to a modified Bradford assay (Ramagli and Rodriguez, 1985).

2-DE

Proteins were first separated according to their charge after passive rehydration of 24-cm-long Immobililine dry strips, pH 4 to 7 (Amersham Biosciences), with 100 μ g of resuspended proteins, 9 μ L immobilized pH gradient buffer, pH 4 to 7, and rehydration buffer (8 M urea, 2% [w/v] CHAPS, 0.3% [w/v] DTT, 2% [v/v] pharmlalyte, pH 3–10), to a final volume of 450 μ L. Isoelectric focusing was performed with Multiphor II (Amersham Biosciences) according to the following program: 2 h at 150 V, 2 h at 400 V, 2 h to increase the voltage from 400 to 3,500 V, 18 h at 3,500 V. After migration, isoelectric focusing strips were stored at -80°C or immediately incubated in equilibration buffer (6 M urea, 50 mM Tris-HCl, pH 8.8, 30% glycerol, 2% [w/v] SDS with addition of 2% [w/v] DTT in the first equilibration step and 2.5% [w/v] iodoacetamide in the second equilibration step, respectively), for 20 min.

SDS-PAGE was carried out with 13% acrylamide gels in the Hoefer Isodalt electrophoresis chamber (45 min at 80 V, 15 h at 120 V).

At least three gels per sample were silver stained (Heukeshoven and Dernick, 1986). Protein spot detection and quantification were obtained using normalized spot volumes given by ImageMaster platinum software, version 5 (Amersham Biosciences) using the total spot volume normalization procedure to discard experimental variations in 2-DE gels between the different stages.

For protein identification by MS, gels were loaded with 600 μ g of protein extract and stained with colloidal Coomassie Blue (Neuhoff et al., 1988).

Protein Identification by MS

For MALDI-TOF analysis, protein spots were excised and digested (Jensen et al., 1999). The excised fragments were washed successively with water, 25 mM ammonium bicarbonate, HPLC-grade acetonitrile/25 mM ammonium

bicarbonate (1:1 [v/v]), and acetonitrile to remove contaminants and destain the proteins. Gel fragments were dried under vacuum on a centrifugal evaporator. Digestion was carried out overnight at 37°C with 10 mL of 0.0125 mg μM L21 trypsin (sequencing grade, modified; Promega) in 25 mM ammonium bicarbonate (pH 7.8). The resulting tryptic fragments were extracted twice with 100 mL of acetonitrile:water (3:2 [v/v]) containing 0.1% trifluoroacetic acid in an ultrasonic bath for 15 min. The pooled supernatants were concentrated to a final volume of approximately 10 μL in a centrifugal evaporator. The tryptic peptides were desalted and concentrated to a final volume of 3 μL with Zip-Tip C_{18} (Millipore), according to the manufacturer's protocol. The matrix of α -cyano-4-hydroxycinnamic acid was prepared at one-half saturation in acetonitrile:water (1:1 [v/v]) acidified with 0.1% trifluoroacetic acid. Each sample (0.8 mL) was mixed with an equal volume of the matrix solution. The mixture was immediately spotted on the MALDI target and allowed to dry and crystallize. The analyses were performed on a BiFlex III MALDI-TOF mass spectrometer (Bruker Daltonics). Reflector spectra were obtained over a mass range of 600 to 3,500 D in the short-pulsed ion extraction mode using an accelerating voltage of 19 kV. Spectra from 100 to 200 laser shots were summed to generate a peptide mass fingerprint for each protein digest. At least two peptide ions generated by the autolysis of trypsin were used as internal standards for calibrating the mass spectra. Automatic monoisotopic mass assignment was performed using Bruker's SNAP procedure. MASCOT search engine software (Matrix Science) was used to search MSDB (version 2002) or TIGR (LeGI, version 9, release July, 2004). The following parameters were used for database searching: (1) mass tolerance of 50 ppm; (2) a minimum of five peptides matching to the protein; and (3) one miscleavage allowed.

For LC-MS/MS analysis, in-gel digestion was performed with a robotic system (Progest; Genomic Solution). After a reduction and alkylation of Cys, trypsin digestion was performed for 5 h with 125 ng of modified trypsin (Promega) diluted in 20 mM ammonium bicarbonate, 20% (v/v) methanol. The resulting peptides were extracted with $2 \times 30 \mu\text{L}$ of 5% (v/v) trifluoroacetic acid, 50% (v/v) acetonitrile. After drying in a vacuum centrifuge, peptide extracts were resuspended in 15 μL of 0.08% (v/v) trifluoroacetic acid, 0.02% (v/v) *n*-heptafluorobutyric acid, and 3% (v/v) acetonitrile prior to LC-MS analysis.

HPLC was performed with the Ultimate LC system combined with Famos autosampler and Switchos II microcolumn switching for preconcentration (Dionex). The samples were loaded on the column (PEPMAP C_{18} , 5 μm , 75 μm i.d., 15 cm; Dionex) using a preconcentration step on a micro precolumn cartridge (300 μm i.d., 5 mm). Four microliters of sample were loaded to a precolumn at 7 $\mu\text{L}/\text{min}$. After 2.5 min, the precolumn was connected with the separating column and the gradient was started at 300 nL/min. Buffers were 0.1% (v/v) acetic acid, 2% (v/v) acetonitrile, and 0.1% (v/v) acetic acid, 95% (v/v) acetonitrile. A linear gradient from 3% to 20% acetonitrile for 25 min was applied. Including the regeneration step, one run was 45 min.

The LCQ Deca XP+ (Thermo Electron) was used with a nanoelectrospray interface. Ionization (1.2–1.6 kV) was performed with liquid junction and a noncoated capillary probe (20 μm i.d.; New Objective).

Peptide ions were analyzed by the *n*th-dependent method as follows: (1) full MS scan (mass-to-charge ratio 400–1,900); (2) ZoomScan (scan of the two major ions with higher resolution); and (3) MS/MS of these two ions ($Q_z = 0.22$, activation time = 50 ms, collision energy = 40%).

Identification was performed with Bioworks 3.1 TM built on SEQUEST algorithm (Eng et al., 1994). The main search parameters were Met oxidation as differential modification, no enzyme as cleavage specificity, EST database translated in the six reading frames (LeGI, TIGR, version 9, release July, 2004). Identification was considered significant when (1) protein was identified with at least three different peptides as first hit; (2) $X_{\text{corr}} > 1.7$, 2.2, and 3.3 for, respectively, mono-, di-, and tricharged peptides, $\delta\text{Cn} > 0.1$, resp < 3 ; and (3) identified peptides were fully tryptic. In a few cases, functional annotation was obtained by blasting the tomato TC sequence on The Arabidopsis Information Resource database.

Statistical Analysis

Spots showing eye-detected variations were submitted to ANOVA to retain the spot for which the stage had a significant effect ($P < 0.05$) on the percent volume of each spot. EPCLUST hierarchical clustering software (available at <http://ep.ebi.ac.uk>) was used to pick out the main classes of variations from the data matrix of mean-centered spot percentage of volumes. Correlation-measured based distances and the UPGMA algorithm were used for the analysis.

ACKNOWLEDGMENTS

We thank Esther Pelpoir for her technical assistance and Jean-Paul Bouchet for his help in managing proteomic data.

Received November 9, 2006; accepted December 20, 2006; published January 5, 2007.

LITERATURE CITED

- Adams-Phillips L, Barry C, Giovannoni J (2004) Signal transduction systems regulating fruit ripening. *Trends Plant Sci* 9: 331–338
- Aharoni A, O'Connell AP (2002) Gene expression analysis of strawberry achene and receptacle maturation using DNA microarrays. *J Exp Bot* 53: 2073–2087
- Alba R, Payton P, Fei Z, McQuinn R, Debbie P, Martin GB, Tanksley SD, Giovannoni JJ (2005) Transcriptome and selected metabolite analyses reveal multiple points of ethylene control during tomato fruit development. *Plant Cell* 17: 2954–2965
- Amemiya T, Kanayama Y, Yamaki S, Yamada K, Shiratake K (2006) Fruit-specific V-ATPase suppression in antisense-transgenic tomato reduces fruit growth and seed formation. *Planta* 223: 1272–1280
- Andrews PK, Fahy DA, Foyer CH (2004) Relationships between fruit exocarp antioxidants in the tomato (*Lycopersicon esculentum*) high pigment-1 mutant during development. *Physiol Plant* 120: 519–528
- Baginsky S, Gruissem W (2006) Arabidopsis thaliana proteomics: from proteome to genome. *J Exp Bot* 57: 1485–1491
- Bertin N (2005) Analysis of the tomato fruit growth response to temperature and plant fruit load in relation to cell division, cell expansion and DNA endoreduplication. *Ann Bot (Lond)* 95: 439–447
- Bertin N, Borel C, Brunel B, Cheniclet C, Causse M (2003) Do genetic make-up and growth manipulation affect tomato fruit size by cell number, or cell size and DNA endoreduplication? *Ann Bot (Lond)* 92: 415–424
- Bertin N, Gautier H, Roche C (2002) Number of cells in tomato fruit depending on fruit position and source-sink balance during plant development. *Plant Growth Regul* 36: 105–112
- Brummell DA, Harpster MH (2001) Cell wall metabolism in fruit softening and quality and its manipulation in transgenic plants. *Plant Mol Biol* 47: 311–339
- Bünger-Kibler S, Bangerth F (1982) Relationship between cell number, cell size and fruit size of seeded fruits of tomato (*Lycopersicon esculentum* Mill.), and those induced parthenocarpically by the application of plant growth regulators. *Plant Growth Regul* 1: 143–154
- Cánovas FM, Dumas-Gaudot E, Recorbet G, Jorin J, Mock HP, Rossignol M (2004) Plant proteome analysis. *Proteomics* 4: 285–298
- Carrari F, Baxter C, Usadel B, Urbanczyk-Wochniak E, Zanon M-I, Nunes-Nesi A, Nikiforova V, Centero D, Ratzka A, Pauly M, et al (2006) Integrated analysis of metabolite and transcript levels reveals the metabolic shifts that underlie tomato fruit development and highlight regulatory aspects of metabolic network behavior. *Plant Physiol* 142: 1380–1396
- Carrari F, Fernie AR (2006) Metabolic regulation underlying tomato fruit development. *J Exp Bot* 57: 1883–1897
- Casado-Vela J, Sellés S, Martínez RB (2005) Proteomic approach to blossom-end rot in tomato fruits (*Lycopersicon esculentum* M.): antioxidant enzymes and the pentose phosphate pathway. *Proteomics* 5: 2488–2496
- Chen G, Hackett R, Walker D, Taylor A, Lin Z, Grierson D (2004) Identification of a specific isoform of tomato lipoxygenase (TomloxC) involved in the generation of fatty acid-derived flavor compounds. *Plant Physiol* 136: 2641–2651
- Cheniclet C, Rong WY, Causse M, Frangne N, Bolling L, Carde JP, Renaudin JP (2005) Cell expansion and endoreduplication show a large genetic variability in pericarp and contribute strongly to tomato fruit growth. *Plant Physiol* 139: 1984–1994
- Clark GB, Sessions A, Eastburn DJ, Roux SJ (2001) Differential expression of members of the annexin multigene family in Arabidopsis. *Plant Physiol* 126: 1072–1084
- da Silva FG, Iandolo A, Al-Kayal F, Bohlmann MC, Cushman MA, Lim H, Ergul A, Figueroa R, Kabuloglu EK, Osborne C, et al (2005) Characterizing the grape transcriptome: analysis of expressed sequence tags

- from multiple vitis species and development of a compendium of gene expression during berry development. *Plant Physiol* **139**: 574–597
- Dai N, German MA, Matsevitz T, Hanael R, Swartzberg D, Yeselson Y, Petreikov M, Schaffer AA, Granot D** (2002) LeFRK2, the gene encoding the major fructokinase in tomato fruits, is not required for starch biosynthesis in developing fruits. *Plant Sci* **162**: 423–430
- Desiere E, Deutsch E, Nesvizhskii A, Mallick P, King N, Eng J, Aderem A, Boyle R, Brunner E, Donohoe S, et al** (2004) Integration with the human genome of peptide sequences obtained by high-throughput mass spectrometry. *Genome Biol* **6**: R9
- Drake R, John I, Farrell A, Cooper W, Schuch W, Grierson D** (1996) Isolation and analysis of cDNAs encoding tomato cysteine proteases expressed during leaf senescence. *Plant Mol Biol* **30**: 755–767
- Duck N, McCormick S, Winter J** (1989) Heat shock protein Hsp70 cognate gene expression in vegetative and reproductive organs of *Lycopersicon esculentum*. *Proc Natl Acad Sci USA* **86**: 3674–3678
- Eng JK, McCormack AL, Yates JR** (1994) An approach to correlate tandem mass spectral data of peptides with amino acid sequences in a protein database. *J Am Soc Mass Spectrom* **5**: 976–989
- Espartero J, Pintor-Toro JA, Pardo JM** (1994) Differential accumulation of S-adenosyl methionine synthetase transcripts in response to salt stress. *Plant Mol Biol* **25**: 217–227
- Faurobert M, Pelpoir E, Chaïb J** (2006) Phenol extraction of proteins for proteomic studies of recalcitrant plant tissues. In M Zivy, ed, *Plant Proteomics. Methods and Protocols*, Vol 355. Humana Press, Totowa, NJ, pp 9–14
- Fei Z, Tang X, Alba RM, White JA, Ronning CM, Martin GB, Tanksley SD, Giovannoni JJ** (2004) Comprehensive EST analysis of tomato and comparative genomics of fruit ripening. *Plant J* **40**: 47–59
- Fernie AR, Trethewey RN, Krotzky AJ, Willmitzer L** (2004) Metabolite profiling: from diagnostics to system biology. *Nat Rev Mol Cell Biol* **5**: 763–769
- Gallardo F, Gálvez S, Gadal P, Cánovas FM** (1995) Changes in NADP⁺-linked isocitrate dehydrogenase during tomato fruit ripening. *Planta* **196**: 148–154
- Galvez S, Lancien M, Hodges M** (1999) Are isocitrate dehydrogenases and 2-oxoglutarate involved in the regulation of glutamate synthesis? *Trends Plant Sci* **4**: 484–490
- Gilbert HF** (1997) Protein disulfide isomerase and assisted protein folding. *J Biol Chem* **272**: 29399–29402
- Gillaspy G, Ben-David H, Gruissem W** (1993) Fruits: a developmental perspective. *Plant Cell* **5**: 1439–1451
- Giovannoni J** (2001) Molecular biology of fruit maturation and ripening. *Annu Rev Plant Physiol Plant Mol Biol* **52**: 725–749
- Giovannoni J** (2004) Genetic regulation of fruit development and ripening. *Plant Cell* **16**: 170–180
- Glaczinski H, Heibges A, Salamini R, Gebhardt C** (2002) Members of the Kunitz-type protease inhibitor gene family of potato inhibit soluble tuber invertase in vitro. *Potato Res* **45**: 163–176
- Grimplet J, Romieu C, Audergon J-M, Marty I, Albagnac G, Lambert P, Bouchet J-P, Terrier N** (2005) Transcriptomic study of apricot fruit (*Prunus armeniaca*) ripening among 13,006 expressed sequence tags. *Physiol Plant* **125**: 281–292
- Gruss OJ, Carazo-Salas RE, Schatz CA, Guarguaglini G, Kast J, Wilm M, Le Bot N, Vernos I, Karsenti E, Mattaj IW** (2001) Ran induces spindle assembly by reversing the inhibitory effect of importin *alpha* on TPX2 activity. *Cell* **104**: 83–93
- Hennig L, Gruissem W, Grossniklaus U, Kohler C** (2004) Transcriptional programs of early reproductive stages in Arabidopsis. *Plant Physiol* **135**: 1765–1775
- Heukeshoven J, Dernick R** (1986) Silver staining of proteins. In BJ Radola, ed, *Electrophoresis Forum*. Technical Munich University, Munich, pp 22–27
- Hieber AD, Bugos RC, Yamamoto HY** (2000) Plant lipocalins: violaxanthin de-epoxidase and zeaxanthin epoxidase. *Biochim Biophys Acta* **1482**: 84–91
- Ho C-L, Saito K** (2001) Molecular biology of the plastidic phosphorylated serine biosynthetic pathway in *Arabidopsis thaliana*. *Amino Acids* **20**: 243–259
- Imin N, Kerim T, Rolfe BG, Weinman JJ** (2004) Effect of early cold stress on the maturation of rice anthers. *Proteomics* **4**: 1873–1882
- Itai A, Ishihara K, Bewley JD** (2003) Characterization of expression, and cloning, of [beta]-D-xylosidase and alpha-L-arabinofuranosidase in developing and ripening tomato (*Lycopersicon esculentum* Mill.) fruit. *J Exp Bot* **54**: 2615–2622
- Iwahashi Y, Hosoda H** (2000) Effect of heat stress on tomato fruit protein expression. *Electrophoresis* **21**: 1766–1771
- Jacob-Wilk D, Goldschmidt EE, Riov J, Sadka A, Holland D** (1997) Induction of a citrus gene highly homologous to plant and yeast thi genes involved in thiamine biosynthesis during natural and ethylene-induced fruit maturation. *Plant Mol Biol* **35**: 661–666
- Jagadeesh BH, Prabha TN, Srinivasan K** (2004) Activities of glycosidases during fruit development and ripening of tomato (*Lycopersicon esculentum* L.): implication in fruit ripening. *Plant Sci* **166**: 1451–1459
- Jensen ON, Wilm M, Shevchenko A, Mann M** (1999) Sample preparation methods for mass spectrometric peptide mapping directly from 2-DE gels. In AJ Link, ed, *Methods in Molecular Biology*, Vol 112. Humana Press, Totowa, NJ, pp 513–530
- Jimenez A, Creissen G, Kular B, Firmin J, Robinson S, Verhoeven M, Mullineaux P** (2002) Changes in oxidative processes and components of the antioxidant system during tomato fruit ripening. *Planta* **214**: 751–758
- Jimenez A, Gomez JM, Navarro E, Sevilla F** (2002) Changes in the antioxidative systems in mitochondria during ripening of pepper fruits. *Plant Physiol Biochem* **40**: 515–520
- Joubès J, Phan TH, Just D, Rothan C, Bergougnieux C, Raymond P, Chevallier C** (1999) Molecular and biochemical characterization of the involvement of cyclin-dependent kinase A during the early development of tomato fruit. *Plant Physiol* **121**: 857–869
- Kang H-C, Lee S-H** (2001) Characteristics of an alpha-galactosidase associated with grape flesh. *Phytochemistry* **58**: 213–219
- Lawrence SD, Cline K, Moore GA** (1997) Chromoplast development in ripening tomato fruit: identification of cDNAs for chromoplast-targeted proteins and characterization of a cDNA encoding a plastid-localized low-molecular-weight heat shock protein. *Plant Mol Biol* **33**: 483–492
- Lemaire-Chamley M, Petit J, Garcia V, Just D, Baldet P, Germain V, Fagard M, Mouassite M, Cheniclet C, Rothan C** (2005) Changes in transcriptional profiles are associated with early fruit tissue specialization in tomato. *Plant Physiol* **139**: 750–769
- Lincoln JE, Cordes S, Read E, Fischer RL** (1987) Regulation of gene expression by ethylene during *Lycopersicon esculentum* (tomato) fruit development. *Proc Natl Acad Sci USA* **84**: 2793–2797
- Lopez AP, Portales RB, Lopez-Raez JA, Medina-Escobar N, Blanco JM, Franco AR** (2006) Characterization of a strawberry late-expressed and fruit-specific peptide methionine sulphoxide reductase. *Physiol Plant* **126**: 129–139
- Löw D, Brändle K, Nover L, Forreiter C** (2000) Cytosolic heat-stress proteins Hsp17.7 class I and Hsp17.3 class II of tomato act as molecular chaperones in vivo. *Planta* **211**: 575–582
- McHale NA, Hanson KR, Zelitch I** (1988) A nuclear mutation in *Nicotiana sylvestris* causing a thiamine-reversible defect in synthesis of chloroplast pigments. *Plant Physiol* **88**: 930–935
- Moffatt BA, Stevens Y, Allen MS, Snider JD, Pereira LA, Todorova MI, Summers PS, Weretilnyk EA, Martin-McCaffrey L, Wagner C** (2002) Adenosine kinase deficiency is associated with developmental abnormalities and reduced transmethylation. *Plant Physiol* **128**: 812–821
- Molhoj M, Verma R, Reiter WD** (2003) The biosynthesis of the branched-chain sugar D-apiose in plants: functional cloning and characterization of a UDP-D-apiose/UDP-D-xylose synthase from Arabidopsis. *Plant J* **35**: 693–703
- Moyle R, Fairbairn DJ, Ripi J, Crowe M, Botella JR** (2005) Developing pineapple fruit has a small transcriptome dominated by metallothionein. *J Exp Bot* **56**: 101–112
- Mueller LA, Solow TH, Taylor N, Skwarecki B, Buels R, Binns J, Lin C, Wright MH, Ahrens R, Wang Y, et al** (2005) The SOL genomics network: a comparative resource for Solanaceae biology and beyond. *Plant Physiol* **138**: 1310–1317
- Neta-Sharir I, Isaacson T, Lurie S, Weiss D** (2005) Dual role for tomato heat shock protein 21: protecting photosystem II from oxidative stress and promoting color changes during fruit maturation. *Plant Cell* **17**: 1829–1838
- Neuhoff V, Arold N, Taube D, Ehrhardt W** (1988) Improved staining of proteins in polyacrylamide gels including isoelectric focusing gels with clear background at nanogram sensitivity using Coomassie Brilliant Blue G-250 and R-250. *Electrophoresis* **9**: 255–262

- Owino WO, Ambuko JL, Mathooko FM (2005) Molecular basis of cell wall degradation during fruit ripening and senescence. *Stewart Postharvest Review*, http://www.stewartpostharvest.com/October_2005/Owino.pdf (October, 2005)
- Papenbrock J, Grimm B (2001) Regulatory network of tetrapyrrole biosynthesis—studies of intracellular signalling involved in metabolic and developmental control of plastids. *Planta* **213**: 667–681
- Park MH, Joe YA, Kang KR (1998) Deoxyhypusine synthase activity is essential for cell viability in the yeast *Saccharomyces cerevisiae*. *J Biol Chem* **273**: 1677–1683
- Penarrubia L, Aguilar M, Margossian L, Fischer RL (1992) An antisense gene stimulates ethylene hormone production during tomato fruit ripening. *Plant Cell* **4**: 681–687
- Peumans WJ, Barre A, Derycke V, Rouge P, Zhang W, May GD, Delcour JA, Van Leuven F, Van Damme EJM (2000) Purification, characterization and structural analysis of an abundant beta-1,3-glucanase from banana fruit. *Eur J Biochem* **267**: 1188–1195
- Pri-Hadash A, Hareven D, Lifschitz E (1992) A meristem-related gene from tomato encodes a dUTPase: analysis of expression in vegetative and floral meristems. *Plant Cell* **4**: 149–159
- Proust J, Houlne G, Schantz M-L, Schantz R (1996) Characterization and gene expression of an annexin during fruit development in *Capsicum annuum*. *FEBS Lett* **383**: 208–212
- Ramagli LS, Rodriguez LV (1985) Quantification of microgram amounts of protein in two dimensional polyacrylamide gel electrophoresis sample buffer. *Electrophoresis* **6**: 559–563
- Ramakrishna W, Deng Z, Ding C-K, Handa AK, Ozminkowski RH Jr (2003) A novel small heat shock protein gene, *vis1*, contributes to pectin depolymerization and juice viscosity in tomato fruit. *Plant Physiol* **131**: 725–735
- Reichheld J-P, Vernoux T, Lardon F, Van Montagu M, Inze D (1999) Specific checkpoints regulate plant cell cycle progression in response to oxidative stress. *Plant J* **17**: 647–656
- Reid JD, Hunter CN (2002) Current understanding of the function of magnesium chelatase. *Biochem Soc Trans* **30**: 643–645
- Rocco M, D'Ambrosio C, Arena S, Faurobert M, Scaloni A, Marra M (2006) Proteomic analysis of tomato fruits from two ecotypes during ripening. *Proteomics* **6**: 3781–3791
- Roessner-Tunali U, Hegemann B, Lytovchenko A, Carrari F, Bruedigam C, Granot D, Fernie AR (2003) Metabolic profiling of transgenic tomato plants overexpressing hexokinase reveals that the influence of hexose phosphorylation diminishes during fruit development. *Plant Physiol* **133**: 84–99
- Rose JKC, Bashir S, Giovannoni JJ, Jahn MM, Saravanan RS (2004) Tackling the plant proteome: practical approaches, hurdles and experimental tools. *Plant J* **39**: 715–733
- Saravanan RS, Rose JKC (2004) A critical evaluation of sample extraction techniques for enhanced proteomic analysis of recalcitrant plant tissues. *Proteomics* **4**: 2522–2532
- Sarry JE, Sommerer N, Sauvage FX, Bergoin A, Rossignol M, Albagnac G, Romieu C (2004) Grape berry biochemistry revisited upon proteomic analysis of the mesocarp. *Proteomics* **4**: 201–215
- Sauter M, Rzewuski G, Marwedel T, Lorbiecke R (2002) The novel ethylene-regulated gene *OsUsp1* from rice encodes a member of a plant protein family related to prokaryotic universal stress proteins. *J Exp Bot* **53**: 2325–2331
- Schauer N, Zamir D, Fernie AR (2005) Metabolic profiling of leaves and fruit of wild species tomato: a survey of the *Solanum lycopersicum* complex. *J Exp Bot* **56**: 297–307
- Seals DE, Randall SK (1997) A vacuole-associated annexin protein, VCaB42, correlates with the expansion of tobacco cells. *Plant Physiol* **115**: 753–761
- Sheoran IS, Olson DJ, Ross ARS, Sawhney VK (2005) Proteome analysis of embryo and endosperm from germinating tomato seeds. *Proteomics* **5**: 3752–3764
- Soh C-P, Ali ZM, Lazan H (2006) Characterisation of an alpha-galactosidase with potential relevance to ripening related texture changes. *Phytochemistry* **67**: 242–254
- Sturm A (1999) Invertases: primary structures, functions, and roles in plant development and sucrose partitioning. *Plant Physiol* **121**: 1–8
- Sun W, Van Montagu M, Verbruggen N (2002) Small heat shock proteins and stress tolerance in plants. *Biochim Biophys Acta* **1577**: 1–9
- Tanaka A, Fujita K, Kikuchi K (1974) Nutrient-physiological studies on the tomato plant. III. Photosynthetic rate on individual leaves in relation to dry matter production of plants. *Soil Sci Plant Nutr* **20**: 173–183
- Terrier N, Glissant D, Grimplet J, Barrieu F, Abbal P, Couture C, Ageorges A, Atanassova R, Léon C, Renaudin J-P, et al (2005) Isogene specific oligo arrays reveal multifaceted changes in gene expression during grape berry (*Vitis vinifera* L.) development. *Planta* **222**: 832–847
- Thompson JE, Hopkins MT, Taylor C, Wang T-W (2004) Regulation of senescence by eukaryotic translation initiation factor 5A: implications for plant growth and development. *Trends Plant Sci* **9**: 174–179
- Van der Hoeven R, Ronning C, Giovannoni J, Martin G, Tanksley S (2002) Deductions about the number, organization, and evolution of genes in the tomato genome based on analysis of a large expressed sequence tag collection and selective genomic sequencing. *Plant Cell* **14**: 1441–1456
- Vierling E (1991) The roles of heat shock proteins in plants. *Annu Rev Plant Physiol Plant Mol Biol* **42**: 579–620
- Wang SY, Jiao H (2001) Changes in oxygen-scavenging systems and membrane lipid peroxidation during maturation and ripening in blackberry. *J Agric Food Chem* **49**: 1612–1619
- Wang T-W, Zhang C-G, Wu W, Nowack LM, Madey E, Thompson JE (2005) Antisense suppression of deoxyhypusine synthase in tomato delays fruit softening and alters growth and development. *Plant Physiol* **138**: 1372–1382
- Watt G, Leoff C, Harper AD, Bar-Peled M (2004) A bifunctional 3,5-epimerase/4-keto reductase for nucleotide-rhamnose synthesis in *Arabidopsis*. *Plant Physiol* **134**: 1337–1346
- Weretilnyk EA, Alexander KJ, Drebenstedt M, Snider JD, Summers PS, Moffatt BA (2001) Maintaining methylation activities during salt stress: the involvement of adenosine kinase. *Plant Physiol* **125**: 856–865
- Wilkinson JQ, Lanahan MB, Conner TW, Klee HJ (1995) Identification of mRNAs with enhanced expression in ripening strawberry fruit using polymerase chain reaction differential display. *Plant Mol Biol* **27**: 1097–1108
- Zegzouti H, Jones B, Frasse P, Marty C, Maitre B, Latche A, Pech J-C, Bouzayan M (1999) Ethylene-regulated gene expression in tomato fruit: characterization of novel ethylene-responsive and ripening-related genes isolated by differential display. *Plant J* **18**: 589–600